ELECTRONIC SUPPLEMENTARY INFORMATION

A Reference Scale of Cucurbit[7]uril Binding Affinities

Mohammad A. Alnajjar,[a] Werner M. Nau*[a] and Andreas Hennig*[a,b]

[a] Department of Life Sciences and Chemistry, Jacobs University Bremen, Campus Ring 1, 28759, Bremen, Germany
[b] Institute of Chemistry of New Materials, Universität Osnabrück, Barbarastr. 7, 49080 Osnabrück, Germany.
* Corresponding author: andreas.hennig@uni-osnabrueck.de and w.nau@jacobs-university.de

Table of Contents

1. Materials and Instrumentation

Materials. Starting materials for synthesis and reference compounds were purchased from Sigma-Aldrich (Steinheim, Germany) or Merck (Mannheim, Germany), and Tokyo Chemical Industry (TCI) and were used without further purification. Deuterated D_2O and DCl for NMR measurements were purchased from Deutero (Kastellaun, Germany), and cucurbit[7]uril (CB7) was purchased from Strem Chemicals Inc. (Massachusetts, United States) or synthesized according to the literature.[1] For titrations in H_2O, water distilled from $KMnO_4$ was used or Millipore water, if not otherwise noted. The compounds (2,3-diazabicyclo[2.2.2]oct-2-enyl) methanamine and aminomethyladamantane-putrescine were synthesized according to literature procedures.[2,3] (*S*)-2-(Adamantan-1-yl)-2-aminoacetic acid hydrochloride was from Ark Pharm Inc. (IL, US). All fluorescence measurements were performed at ambient temperature using PMMA cuvettes, if not noted otherwise. The counterion for all compounds was chloride, if not noted otherwise.

Instrumentation. ^{1}H NMR spectra were recorded on a JEOL ECX 400 spectrometer. Fluorescence was measured with a Varian Eclipse spectrofluorimeter. ITC experiments were carried out on a VP-ITC from Microcal Inc. (Northampton, MA, United States) at 25 °C. The solutions were degassed and thermostatted by a ThermoVac accessory for ITC experiments. pH values were measured with a Weilheim 3110 pH meter. The pH was converted to pD by the known relation (+ 0.40 units).[4]

2. Abbreviations

ADA: adamantylamine, AMADA: aminomethyladamantane, AMADA-aa: (*S*)-2-(adamantan-1-yl)-2-aminoacetic acid hydrochloride, AMADA-Put: *N*-(adamantylmethyl)butane-1,4-diamine, BE: berberine chloride, BODIPY: 4,4-difluoro-4-bora-3a,4a-diaza-s-indacene, CB7: cucurbit[7]uril, CBAMC: *cis*-1,4-bis(aminomethyl)-cyclohexane, CHMA: cyclohexylmethylamine, DBO-A: (2,3-diazabicyclo[2.2.2]oct-2-enyl) methylamine, FDMA: *N*,*N*-dimethylaminomethylferrocene, HMD: hexamethylenediamine, ITC: isothermal titration calorimetry, NMR: nuclear magnetic resonance spectroscopy, Put: putrescine, PXD: *p*-xylylenediamine, TBA: tetrabutylammonium chloride, TBAMC: *trans*-1,4-bis(aminomethyl)-cyclohexane.

3. Binding Constant Determinations and Error Calculations

In general, the error Δy of a function $y = f(x_1, x_2,\ldots,x_n)$, which is dependent on more than one independent value and its respective error ($\Delta x_1, \Delta x_2,\ldots, \Delta x_n$), is given by:

$$\Delta y = \sqrt{\left(\frac{\partial y}{\partial x_1}\right)^2 \Delta x_1^2 + \left(\frac{\partial y}{\partial x_2}\right)^2 \Delta x_2^2 + \ldots + \left(\frac{\partial y}{\partial x_n}\right)^2 \Delta x_n^2} \quad (1)$$

3.1 Determination of Reference Values and Their Uncertainty

To determine the final binding constant reference value from *n* different binding constants, which have been determined by various methods (e.g. NMR, fluorescence, and ITC), we first, determined the average by:

$$K_{a,ave} = \frac{K_{a,1} + K_{a,2} + \ldots + K_{a,n}}{n} \quad (2)$$

Then, the respective error for the average value is given by considering the errors of the different binding constants by:

$$\Delta K_{a,ave} = \sqrt{\frac{1}{n^2}\left(\Delta K_{a,1}^{\ 2} + \Delta K_{a,2}^{\ 2} + \ldots + \Delta K_{a,n}^{\ 2}\right)} \quad (3)$$

As a specific example, the binding constant of BE was determined by NMR, ITC, and fluorescence as (2.40 ± 0.22) × 10^7 M^{-1}, (2.26 ± 0.39) × 10^7 M^{-1}, and (2.43 ± 0.39) × 10^7 M^{-1}. Then, the proposed value for the binding constant reference values is $K_{a,ave} = \frac{(2.40 + 2.26 + 2.43) \times 10^7 M^{-1}}{3} = 2.36 \times 10^7 M^{-1}$ and the respective error is

$$\Delta K_{a,ave} = \sqrt{\frac{1}{3^2}\left(\left(0.22 \times 10^7 M^{-1}\right)^2 + \left(0.39 \times 10^7 M^{-1}\right)^2 + \left(0.39 \times 10^7 M^{-1}\right)^2\right)} = 0.20 \times M^{-1}$$

.

3.2 Error Propagation for Fluorescence Displacement Titrations

Fluorescence displacement titrations were analysed with OriginLab OriginPro 2020 as previously described.[5] Here, we now used the global fitting routine implemented in

OriginPro to simultaneously analyse more than one binding titration at the same time to obtain the best fit for all analysed binding titration curves. Unfortunately, the uncertainty of the reference binding constant value of the fluorescent dye could not be implemented in the OriginPro fitting procedure. To assess the uncertainty in a different way, the data was analysed twice considering the upper and lower limits of the error of the reference value. Herein, the proposed reference value for BE is K_a = (2.36 ± 0.20) × 10^7 M^{-1}, such that the displacement titration data was analysed twice with a fixed binding constant parameter for BE of $K_{a,BE}$ = (2.36 + 0.20) × 10^7 M^{-1} = 2.56 × 10^7 M^{-1} and $K_{a,BE}$ = (2.36 – 0.20) × 10^7 M^{-1} = 2.16 × 10^7 M^{-1}. This gave two different binding constants of the competitor and a respective error, ($K_{a,max} \pm \Delta K_{a,max}$) and ($K_{a,min} \pm \Delta K_{a,min}$).

Then, the binding constant value of the competitor, $K_{a,C}$, for the fluorescence displacement titration was obtained by considering the upper end and lower limits of the range given by this procedure:

$$K_{a,C} = \frac{\left(\left(K_{a,max} + \Delta K_{a,max}\right) + \left(K_{a,min} - \Delta K_{a,min}\right)\right)}{2} \quad (4)$$

The error of the binding constant was then calculated by:

$$\Delta K_{a,C} = \frac{\Delta K_{a,max} + \Delta K_{a,min}}{2} \quad (5)$$

As a specific example, the value of the binding constant for the reference compound PXD by fluorescence displacement titrations was obtained by global fitting of six fluorescence displacement using a competitive binding titration function.[6] The data was then analysed twice using a binding constant for BE of 2.56 × 10^7 M^{-1} and 2.16 × 10^7 M^{-1}, which gave the values shown in **Table S1**.

Table S1. Binding constants of BE used as fixed parameters in the global fitting procedure of the fluorescence displacement titrations for determining the binding constant of PXD and its error by global fitting.

$K_{a,BE}$ / × 10^7 M^{-1}	2.56	2.16
$K_{a,PXD}$/ × 10^{10} M^{-1}	2.17 ± 0.18	1.79 ± 0.14

The binding constant value of the competitor PXD was then $K_{a,C}$ = ½ × [(2.17 + 0.18) × 10^{10} M^{-1} + 1.79 − 0.14) × 10^{10} M^{-1}] = 2.00 × 10^{10} M^{-1} and the error was $\Delta K_{a,C}$ = 0.35 × 10^{10} M^{-1} (see also Table 1 in main text). Note that this covers the whole range of binding constants, namely

the maximum binding constant ((2.17 + 0.18) × 10^{10} M^{-1} = 2.35 × 10^{10} M^{-1}) and the minimum binding constant ((1.79 – 0.14) × 10^{10} M^{-1} = 1.65 × 10^{10} M^{-1}).

3.3 Error Propagation and Binding Constants by Competitive NMR

3.3.1 Relative Binding Constants by Competitive NMR

K_{rel} is the ratio of the binding constants of a reference compound, $K_{a,ref}$, and a competitor, $K_{a,C}$, where $[Ref]_{free}$ is the free concentration of the reference compound, $[C]_{free}$ is the free concentration of the competitor, and [CB7•Ref] and [CB7•C] are the concentrations of the respective CB7 complexes (eq. 6).

$$K_{rel} = \frac{K_{a,C}}{K_{a,ref}} = \frac{[CB7{\bullet}C][Ref]_{free}}{[CB7{\bullet}Ref][C]_{free}} \tag{6}$$

The concentrations can be calculated by eqs. 7-10 using the integrated peak areas of the ^{1}H NMR signals of the free reference, $I_{free,ref}$, the bound reference, $I_{bound,ref}$, the bound competitor, $I_{bound,C}$, the free competitor, $I_{free,C}$, as well as the total concentrations of reference, $[Ref]_{total}$, and the competitor, $[C]_{total}$.

$$[CB7{\bullet}Ref] = \frac{I_{bound,ref}}{I_{bound,ref} + I_{free,ref}} \times [Ref]_{total} \tag{7}$$

$$[Ref]_{free} = \frac{I_{free,ref}}{I_{bound,ref} + I_{free,ref}} \times [Ref]_{total} \tag{8}$$

$$[CB7{\bullet}C] = \frac{I_{bound,C}}{I_{bound,C} + I_{free,C}} \times [C]_{total} \tag{9}$$

$$[C]_{free} = \frac{I_{free,C}}{I_{bound,C} + I_{free,C}} \times [C]_{total} \tag{10}$$

Combining equations 6-10 gives:

$$K_{rel} = \frac{I_{bound,C} \times I_{free,ref}}{I_{free,C} \times I_{bound,ref}} \tag{11}$$

This procedure was repeated n times ($n \geq 3$) by evaluating different peaks in the same NMR spectrum and gave an average binding constant according to eq. 2 and its error as the standard deviation (eq. 12):

$$\Delta K_{rel} = \sqrt{\frac{\sum_n (K_{rel,n} - K_{rel,ave})}{(n-1)}} \tag{12}$$

In those cases, in which no well-resolved NMR signals could be obtained, the concentrations were calculated using the law of mass conservation (equations 13-15), where $[CB7]_{total}$ is the total concentration of CB7.

$$[C]_{total} = [C]_{free} + [CB7{\bullet}C] \quad (13)$$

$$[Ref]_{total} = [Ref]_{free} + [CB7{\bullet}Ref] \quad (14)$$

$$[CB7]_{total} = [CB7{\bullet}C] + [CB7{\bullet}Ref] \quad (15)$$

3.3.2 Absolute Binding Constants by Competitive NMR

With the known binding constant of the reference compound, the absolute binding constant of the competitor was then calculated by rearranging eq. 6, which gives eq. 16:

$$K_{a,C} = K_{rel} \times K_{a,ref} \quad (16)$$

The respective error was calculated using standard rules of error propagation (see eqs. 1 and 16), which gave eq. 17, where $\Delta K_{a,ref}$ is the error of $K_{a,ref}$ (obtained as described in Section SI 3.1), and $\Delta K_{a,C}$ is the resulting error of $K_{a,C}$.[7]

$$\Delta K_{a,C} = \sqrt{K_{rel}^2 \times (\Delta K_{a,ref})^2 + K_{a,ref}^2 \times (\Delta K_{rel})^2} \quad (17)$$

Eq. 17 is then combined with eq. 16 to give eq. 18:

$$\Delta K_{a,C} = K_{a,C} \times \sqrt{\left(\frac{\Delta K_{a,ref}}{K_{a,ref}}\right)^2 + \left(\frac{\Delta K_{rel}}{K_{rel}}\right)^2} \quad (18)$$

3.3.3 Example of Binding Constant and Error Determinations by NMR

To obtain the relative affinity of different CB7 guest pairs, we measured the concentrations of each of the CB7•guest complexes and the concentration of each free guest. The concentration of CB7 is limiting quantity for all measurements. From eqs. 7-10 and 13-15, it becomes apparent that the equilibrium concentrations of all species can be individually calculated after integrating the relevant peaks. Within experimental restrictions, e.g. limited compound solubility or complex precipitation, the ratio of the integrated peak areas could be adjusted to easily integratable values by carefully selecting the concentrations of the reference and the competing guest.

As an example, we provide in the following details on the determination of the binding constant and its error of BE using Put as a reference compound. From eq. 16, we obtain in this case eq. 19:

$$K_{rel} = \frac{K_{a,BE}}{K_{a,Put}} = \frac{[CB7{\bullet}BE][Put]}{[BE][CB7{\bullet}Put]} \tag{19}$$

Using the law of mass conservation:

$$[Put] = [Put]_{tot} - [CB7{\bullet}Put] \tag{20}$$

and

$$[CB7{\bullet}Put] = [CB7]_{tot} - [CB7{\bullet}BE] \tag{21}$$

gives

$$K_{rel} = \frac{[CB7{\bullet}BE]\left([Put]_{tot} - [CB7]_{tot} + [CB7{\bullet}BE]\right)}{[BE]\left([CB7]_{tot} - [CB7{\bullet}BE]\right)} \tag{22}$$

The concentration of the CB7/BE complex can be determined by eq. 9, in which BE is the competitor, which gives

$$[CB7{\bullet}BE] = \frac{I_{CB7{\bullet}BE}}{I_{CB7{\bullet}BE} + I_{BE}}[BE] \tag{23}$$

Four K_{rel} values were then obtained for each measured spectrum (see Tables S2-S4) by using the integrated peak areas of the peaks labelled as 1 (= I_{BE}) and 1' (= $I_{CB7{\bullet}BE}$), 2 (= I_{BE}) and 2' (= $I_{CB7{\bullet}BE}$), 3 (= I_{BE}) and 3' (= $I_{CB7{\bullet}BE}$), and 5+11 (= I_{BE}) and 5'+11' (= $I_{CB7{\bullet}BE}$) (see Fig. 2 in main text and Fig. S5 for peak assignment). The K_{rel} value and its error for each spectrum was then calculated as the average (eq. 2) and standard deviation (eq. 12) of these four K_{rel} values.

Table S2. Integrated peak areas of the proton signals used to calculate K_{rel} of BE against Put (Measurement No. 1, refers to the NMR spectrum shown in Figure 2 in the main text). K_{rel} = 12.50 ± 0.57.

Proton signal used	$I_{free,C}$	$I_{bound,C}$	K_{rel}
5 + 11	0.62	0.12	12.74
2	0.31	0.61	13.16
1	0.62	1.16	11.91
3	0.64	1.21	12.16

Table S3. Integrated peak areas of the proton signals used to calculate K_{rel} of BE against Put (Measurement No. 2, spectrum not shown). K_{rel} = 13.25 ± 1.54.

Proton signal used	$I_{free,C}$	$I_{bound,C}$	K_{rel}

5 + 11	0.64	1.12	13.91
2	0.32	0.49	11.02
1	0.63	1.08	13.53
3	0.64	1.14	14.52

Table S4. Integrated peak areas of the proton signals used to calculate K_{rel} of BE against Put (Measurement No. 3, spectrum not shown). $K_{rel} = 13.82 \pm 0.71$.

Proton signal used	$I_{free,C}$	$I_{bound,C}$	K_{rel}
5 + 11	0.64	1.04	13.7
2	0.34	0.52	13.7
1	0.69	1.03	13.1
3	0.67	1.07	14.8

Then, the average of the K_{rel} values of all three spectra was calculated by eq. 2, which gave $K_{rel} = 13.18$ and the error by eq. 3, which gave $\Delta K_{rel} = 0.60$. This was then converted (eq. 16 and 18) into the absolute binding constant of BE by competitive NMR, $K_{a,BE} = (2.40 \pm 0.22) \times 10^7$ M^{-1}.

4. Supporting Results

4.1 Berberine Chloride (BE)

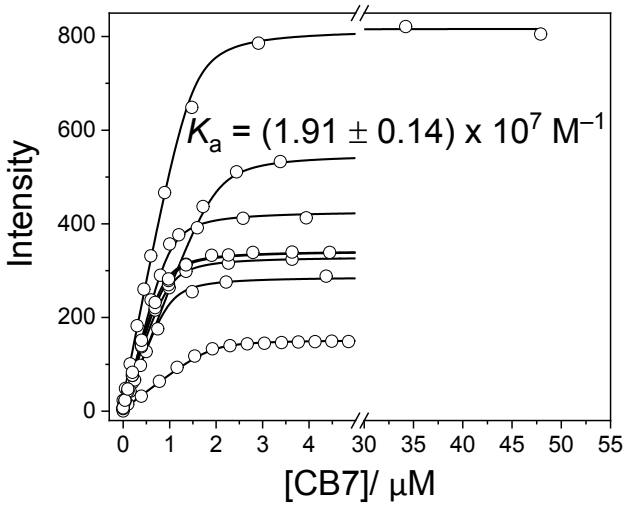

Fig. S1 Fluorescence titration plots (λ_{ex} = 420 nm; λ_{em} = 490 nm) of different BE concentrations (1-2 μM) upon addition of CB7 at pH 7.0. The data was obtained by different individuals in our lab during the previous years with different commercial and self-synthesized CB7 batches. Herein, the data is re-evaluated by a global fitting procedure, which provides the best fit to all titrations as well as the respective error.

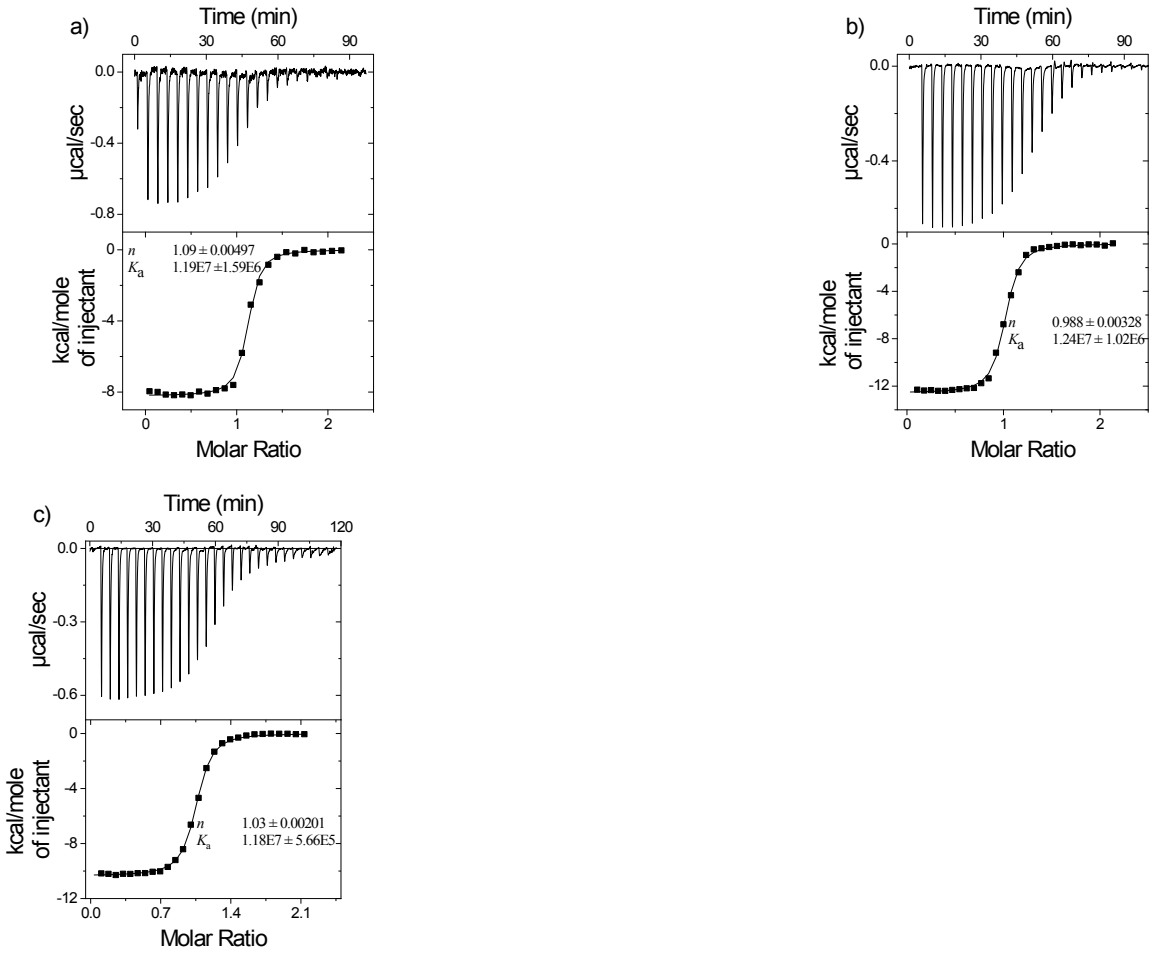

Fig. S2 ITC titration isotherms of varying CB7 concentrations (14 µM (a), 20 µM (b), and 15 µM (c)) upon addition of BE in H_2O, pH 7.0 at 25 °C.

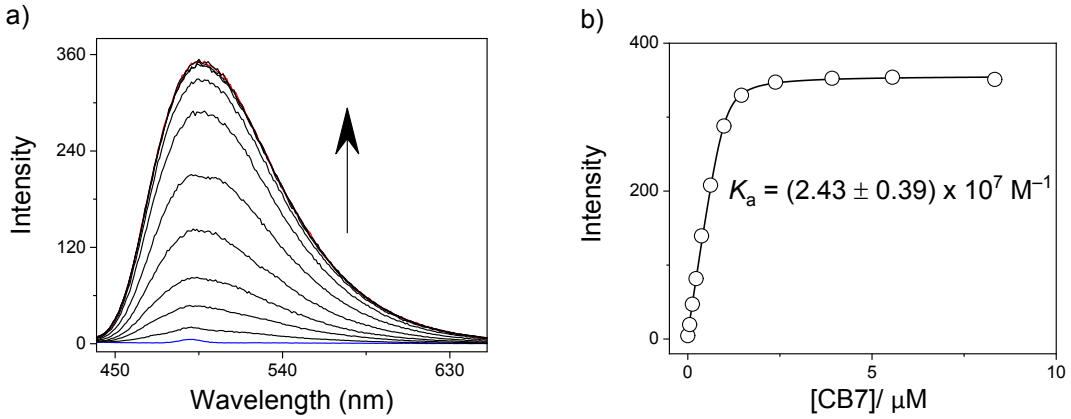

Fig. S3 a) Fluorescence spectral changes (λ_{ex} = 420 nm) of 1.0 µM BE upon addition of CB7 at pH 7.0 in water distilled from $KMnO_4$. b) Respective titration plot (λ_{em} = 490 nm).

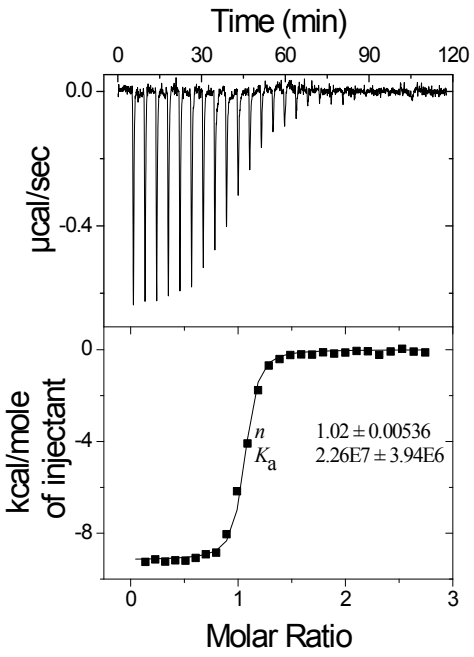

Fig. S4 ITC isotherms on complexation of 14 µM CB7 with BE measured in water distilled from $KMnO_4$, pH 7.0, 25 °C.

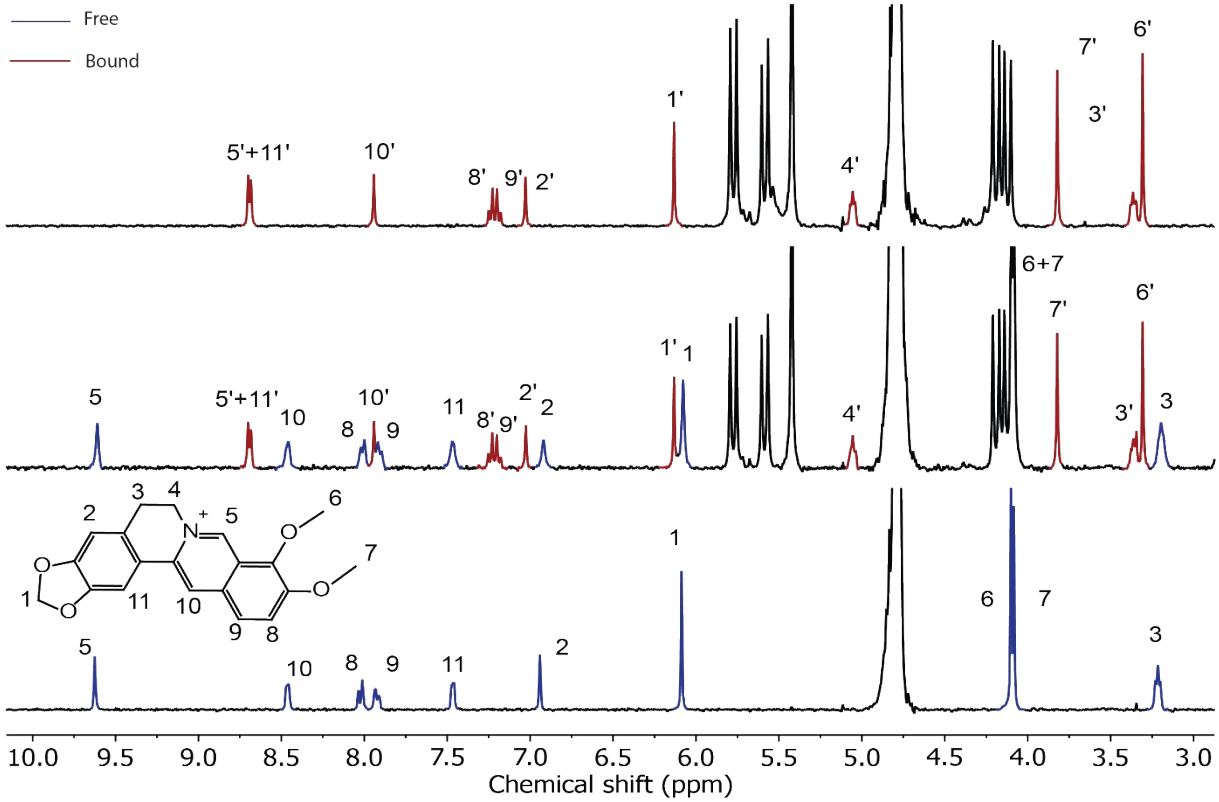

Fig. S5 ^{1}H NMR spectra of 2 mM BE (bottom), 1 mM BE with 0.5 mM CB7 (middle), and 1 mM BE with 1 mM CB7 (top).

4.2 Hexamethylenediamine (HMD)

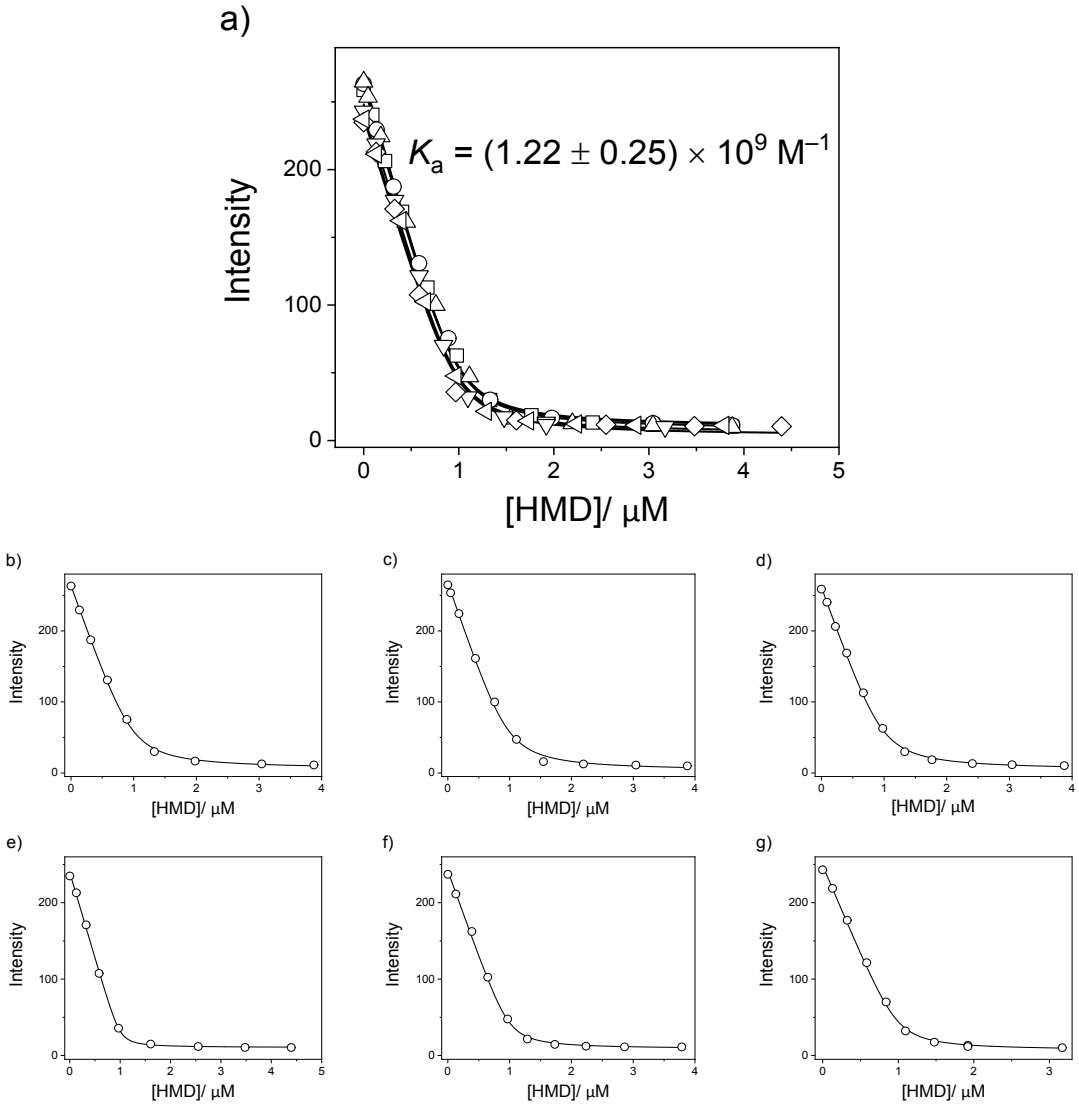

Fig. S6 a) 1:1 Global fitting of the titration plots shown in Panels b-g. b-g) Titration plots obtained from the fluorescence spectral changes (λ_{ex} = 420 nm, λ_{em} = 490 nm) of 2.0 μM BE and 1.0 μM CB7 upon addition of HMD at pH 7.0 using Millipore water in b), c), and d), water distilled from $KMnO_4$ in e), f), and g). Note that the shape of the titration curves was independent on the type of water used. Consequently, the global fitting (Panel a) included data with both types of water, but used the reference K_a value of BE in water distilled from $KMnO_4$ (see also main text).

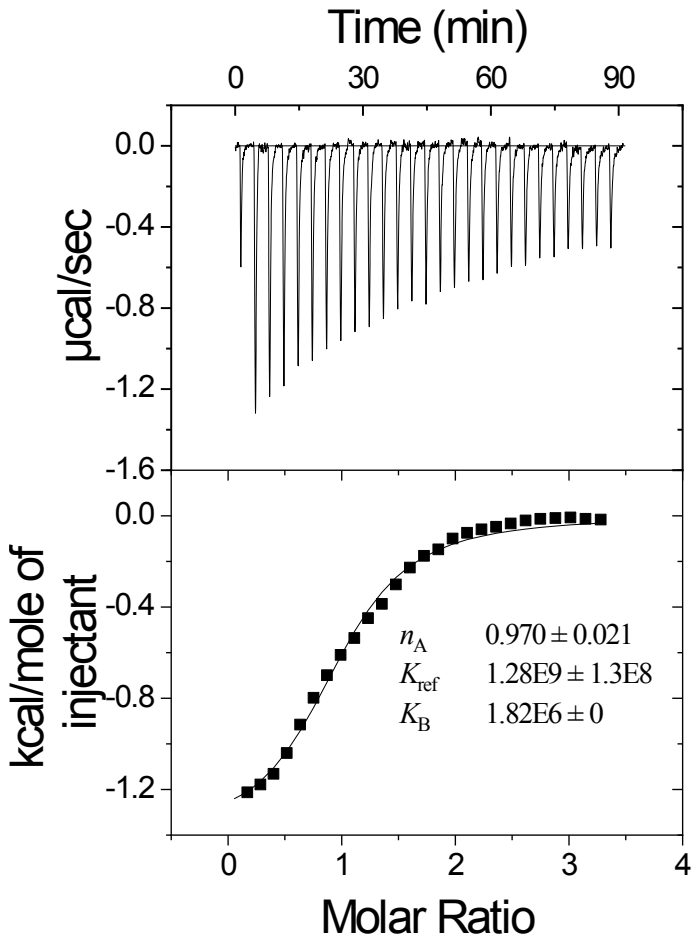

Fig. S7 Competition ITC isotherms on complexation of 100 µM CB7 with HMD in the presence of 10 mM Put in H_2O, pH 7.0 at 25 °C.

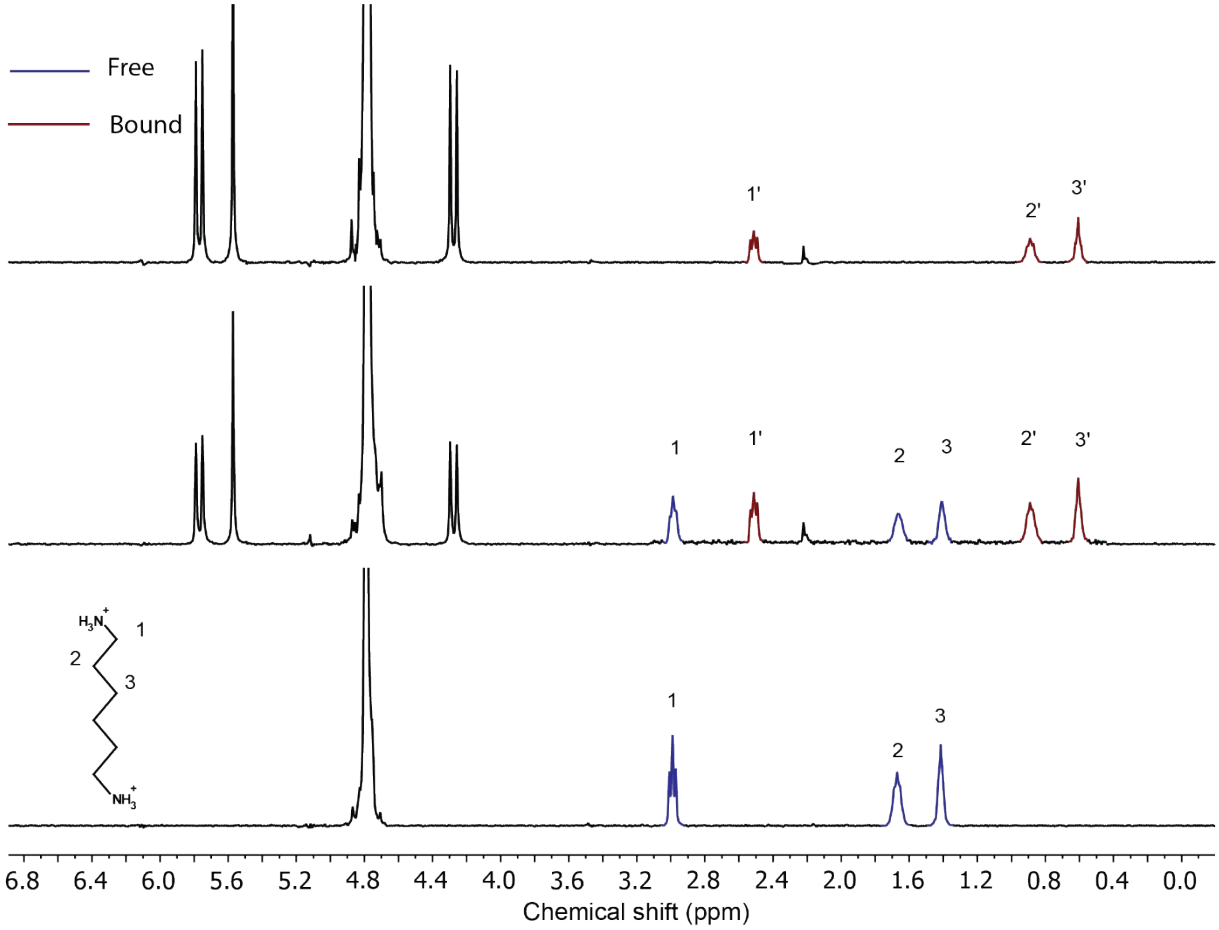

Fig. S8 ^{1}H NMR spectra for 2 mM HMD (bottom), 1 mM HMD with 0.5 mM CB7 (middle), and 1 mM HMD with 1 mM CB7 (top).

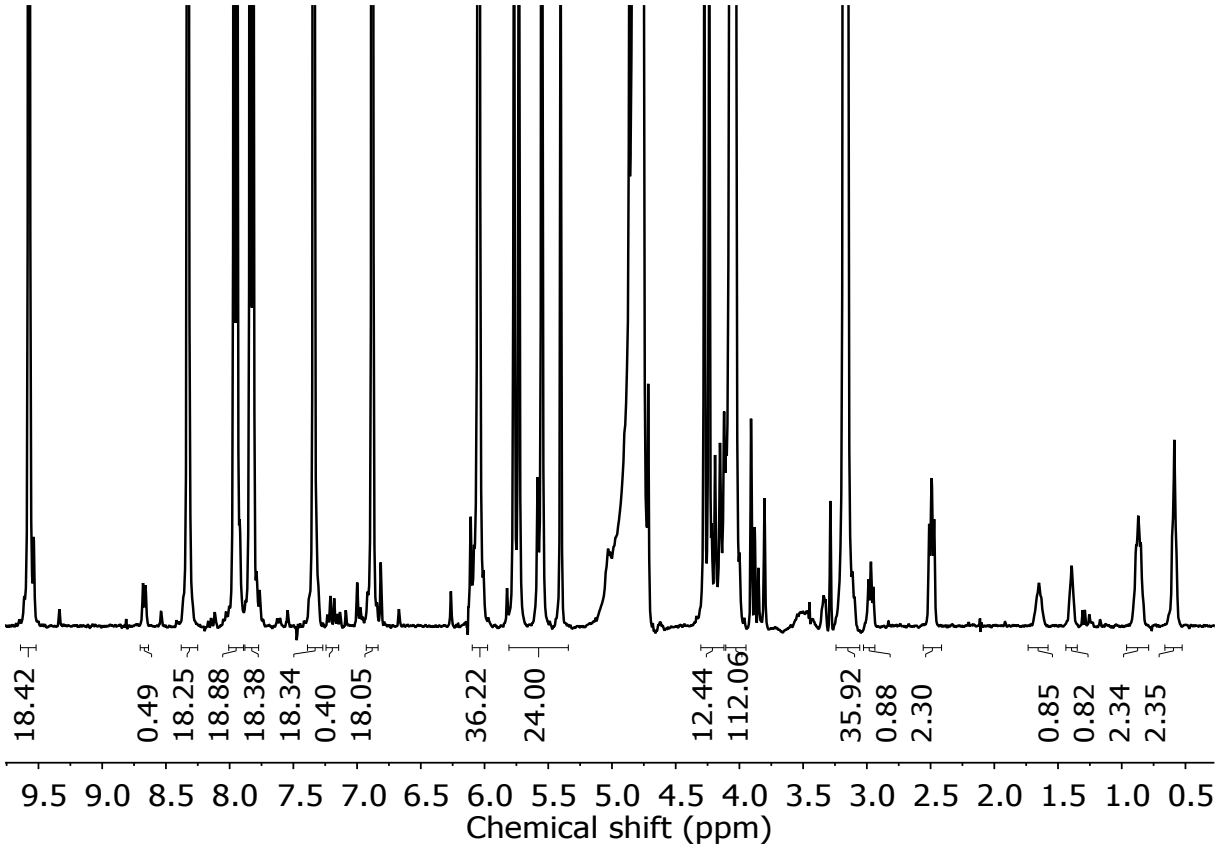

Fig. S9 ^{1}H NMR spectra used to determine the K_{rel} for **BE**•CB7 and **HMD**•CB7 in D_2O at pD 7.4. Concentrations were 2 mM BE, 100 μM HMD and 100 μM CB7.

4.3 *p*-Xylylenediamine (PXD)

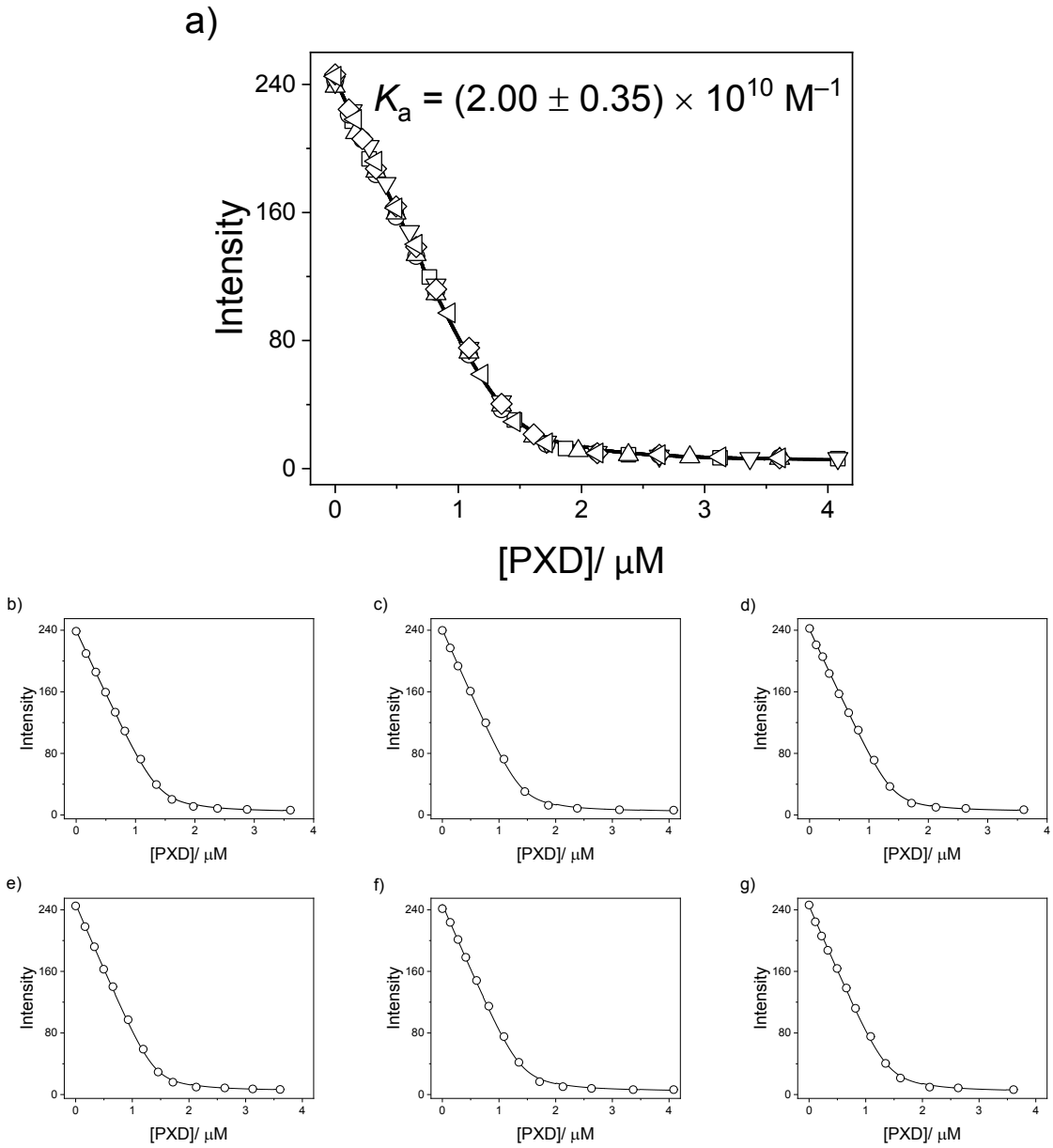

Fig. S10 a) Global fitting of the titration plots shown in Panels b-g. b-g) Titration plots obtained from the fluorescence spectral changes (λ_{ex} = 420 nm, λ_{em} = 490 nm) of 25.0 μM BE and 1.4 μM CB7 upon addtion of PXD at pH 7.0. Millipore water was used in b), c) and d), and water distilled from $KMnO_4$ in e), f) and g).

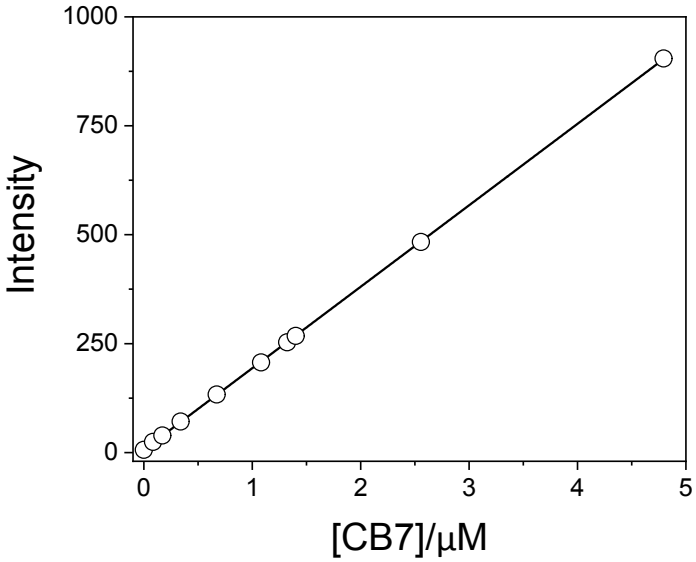

Fig. S11 Linear response of the flourescence intensity of 25 μM BE in a 10×4 mm quartz glass cuvette towards CB7 addition.

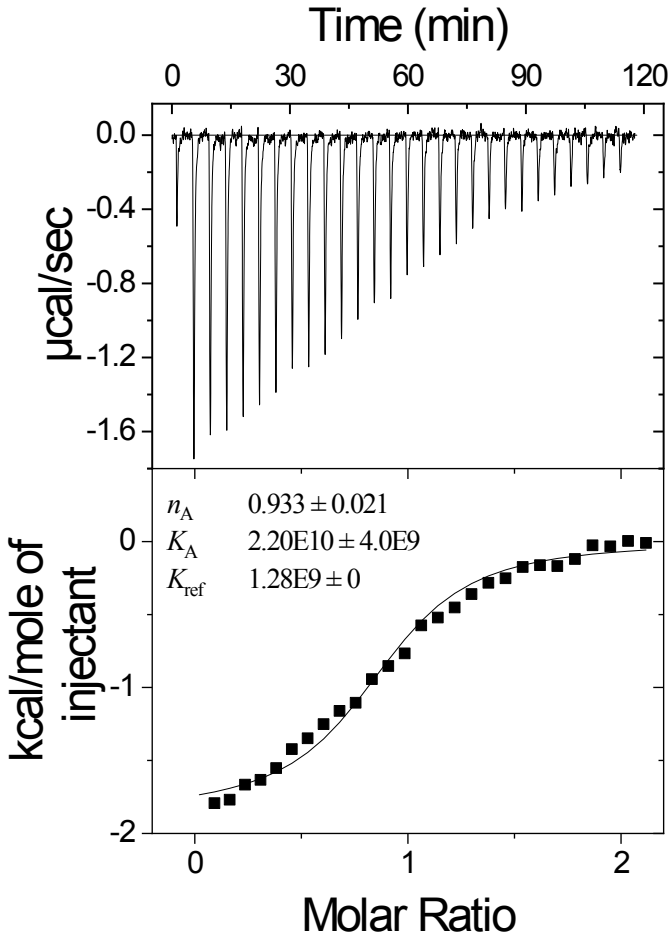

Fig. S12 Competition ITC isotherms on complexation of 250 μM CB7 with PXD in the presence of 250 μM HMD in H_2O, pH 7.0 at 25 °C.

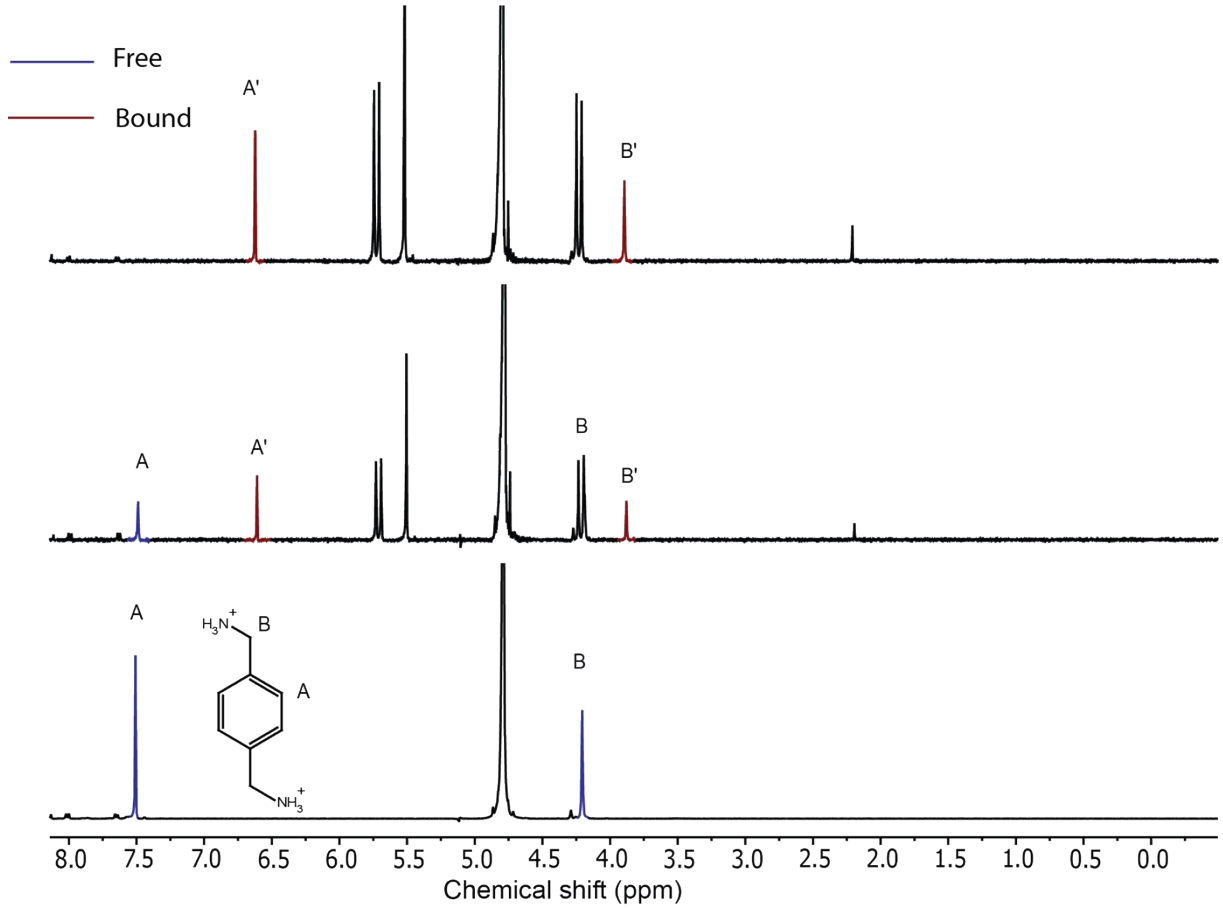

Fig. S13 ^{1}H NMR spectra for 2 mM PXD (bottom), 1 mM PXD with 0.5 mM CB7 (middle), and 1 mM PXD with 1 mM CB7 (top).

4.4 Putrescine (Put)

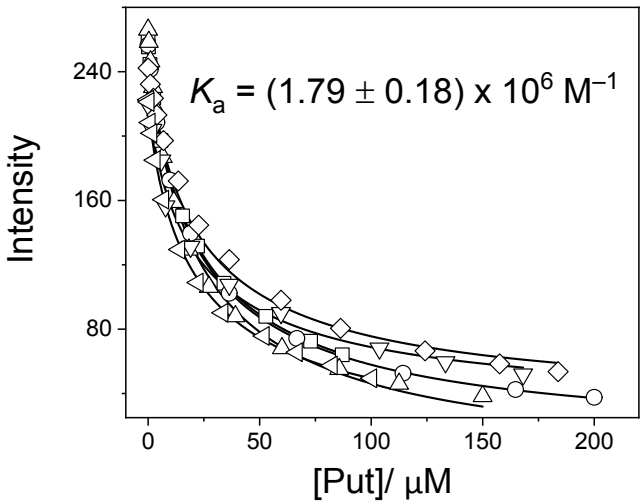

Fig. S14 Global fitting of titration plots obtained from the fluorescence spectral changes (λ_{em} = 490, λ_{ex} = 420 nm nm) of 2.0 μM BE and 1.0 μM CB7 upon addition of Put at pH 7.0 using Millipore water and water distilled from $KMnO_4$.

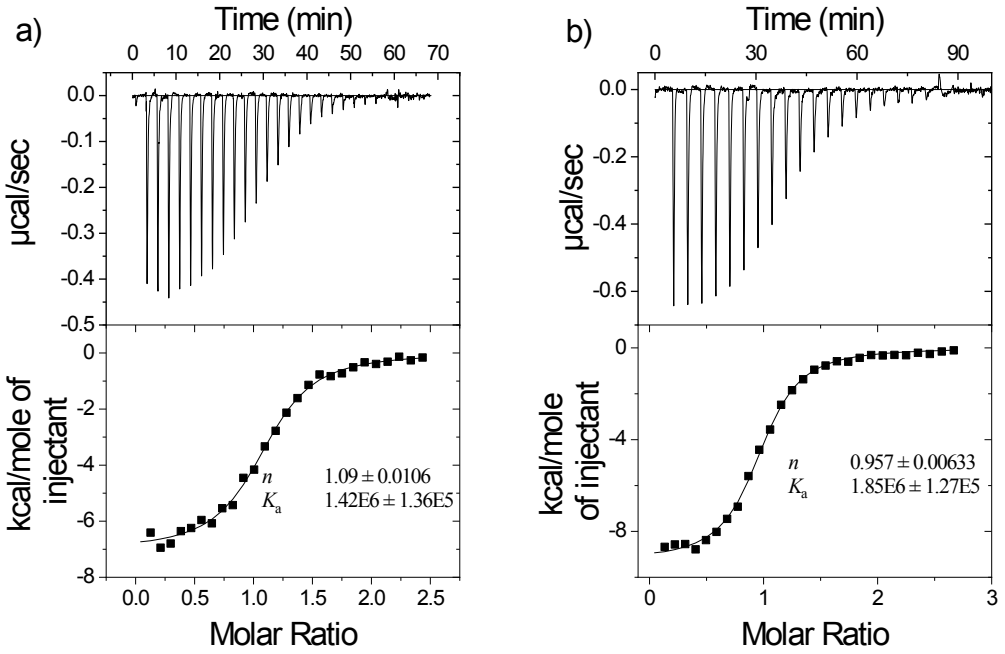

Fig. S15 ITC isotherms on complexation of Put with a) 16 μM CB7 in Millipore water b) 20 μM CB7 in water distilled from $KMnO_4$, at pH 7.0, 25 °C.

4.5 Tetrabutylammonium chloride (TBA)

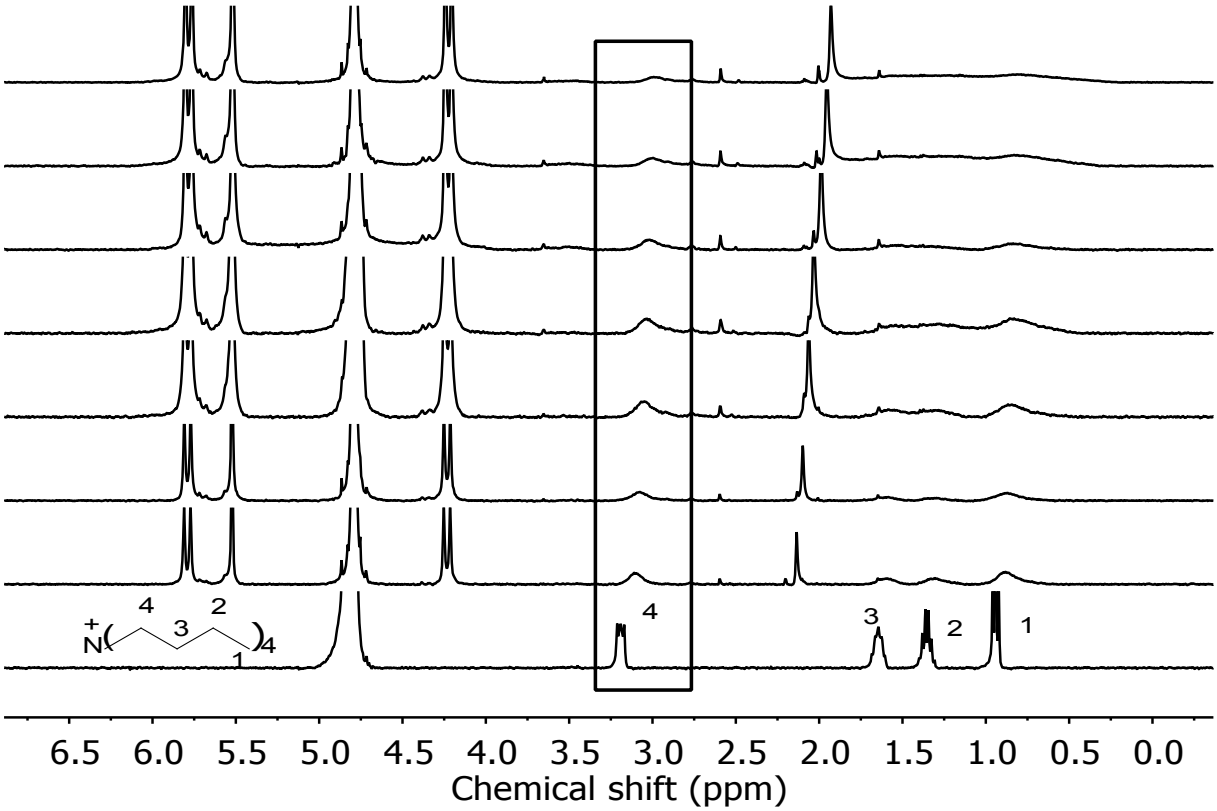

Fig. S16 ^{1}H NMR titration spectra for 300 μM TBA with different (See Fig. S17) CB7 concentrations at pD 7.4.

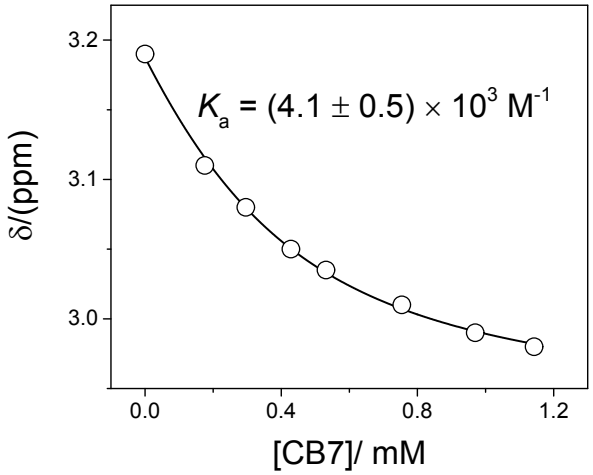

Fig. S17 ^{1}H NMR chemical shift changes of the TBA proton signal (300 μM) at δ = 3.19 ppm upon addition of CB7 at pD 7.4.

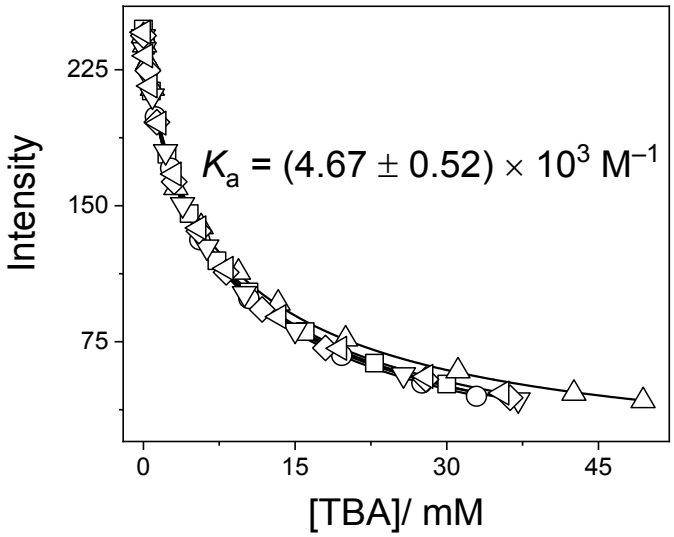

Fig. S18 1:1 Global fitting of titration plots obtained from the fluorescence spectral changes (λ_{em} = 490, λ_{ex} = 420 nm nm) of 1.8 µM BE and 1.0 µM CB7 upon addition TBA at pH 7.0 using Millipore water and water distilled from $KMnO_4$.

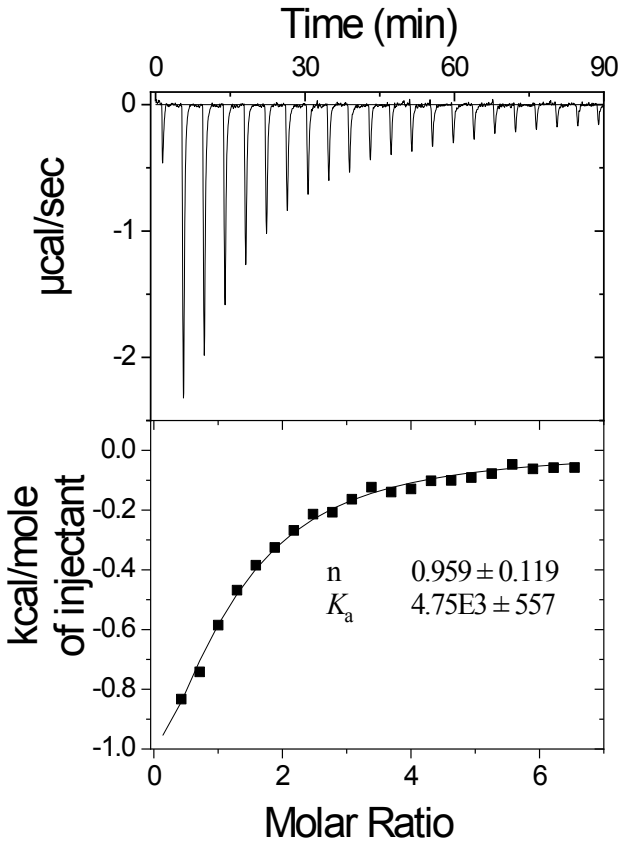

Fig. S19 ITC isotherms on complexation of 200 µM CB7 with TBA measured in H_2O pH 7.0, 25 °C.

4.6 Cyclohexylmethylamine (CHMA)

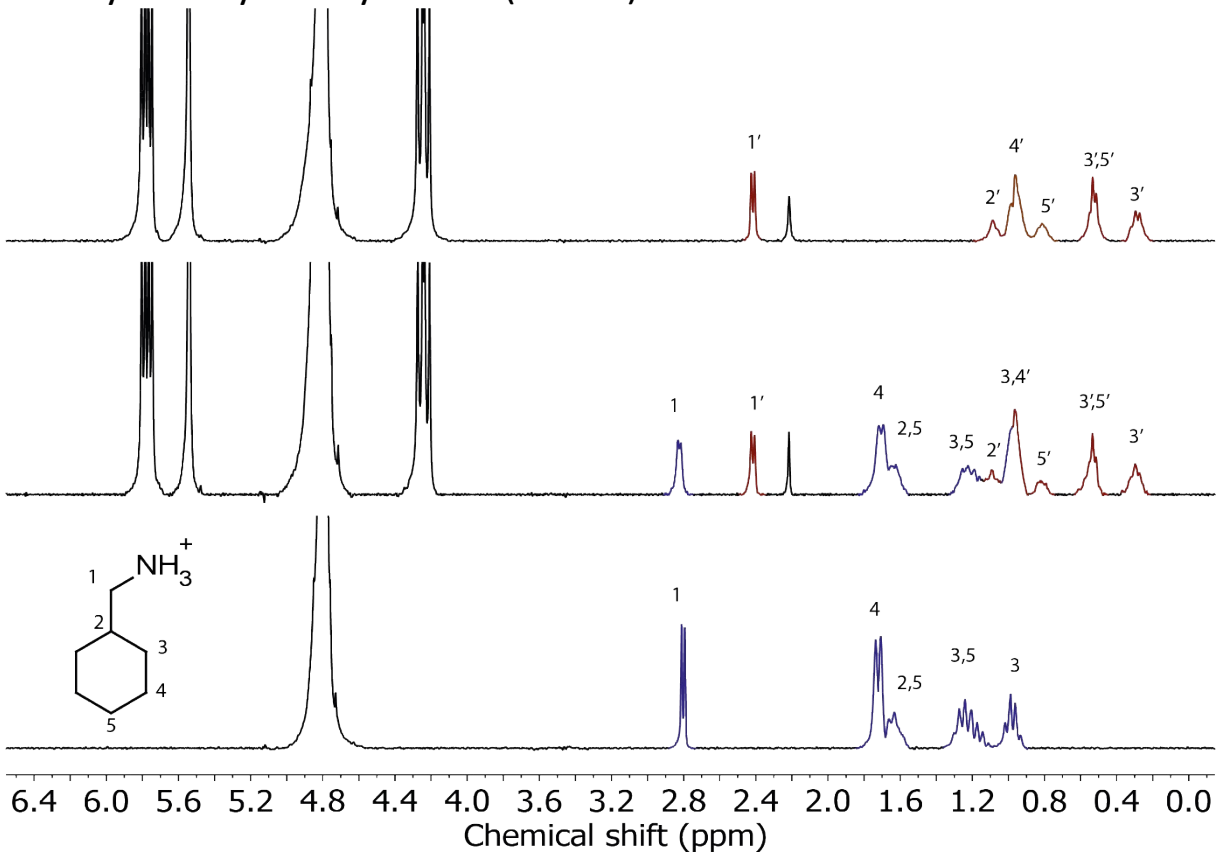

Fig. S20 ^{1}H NMR spectra for 2 mM CHMA free (bottom), 1 mM CHMA with 0.5 mM CB7 (middle), and 1 mM CHMA with 1 mM CB7 (top).

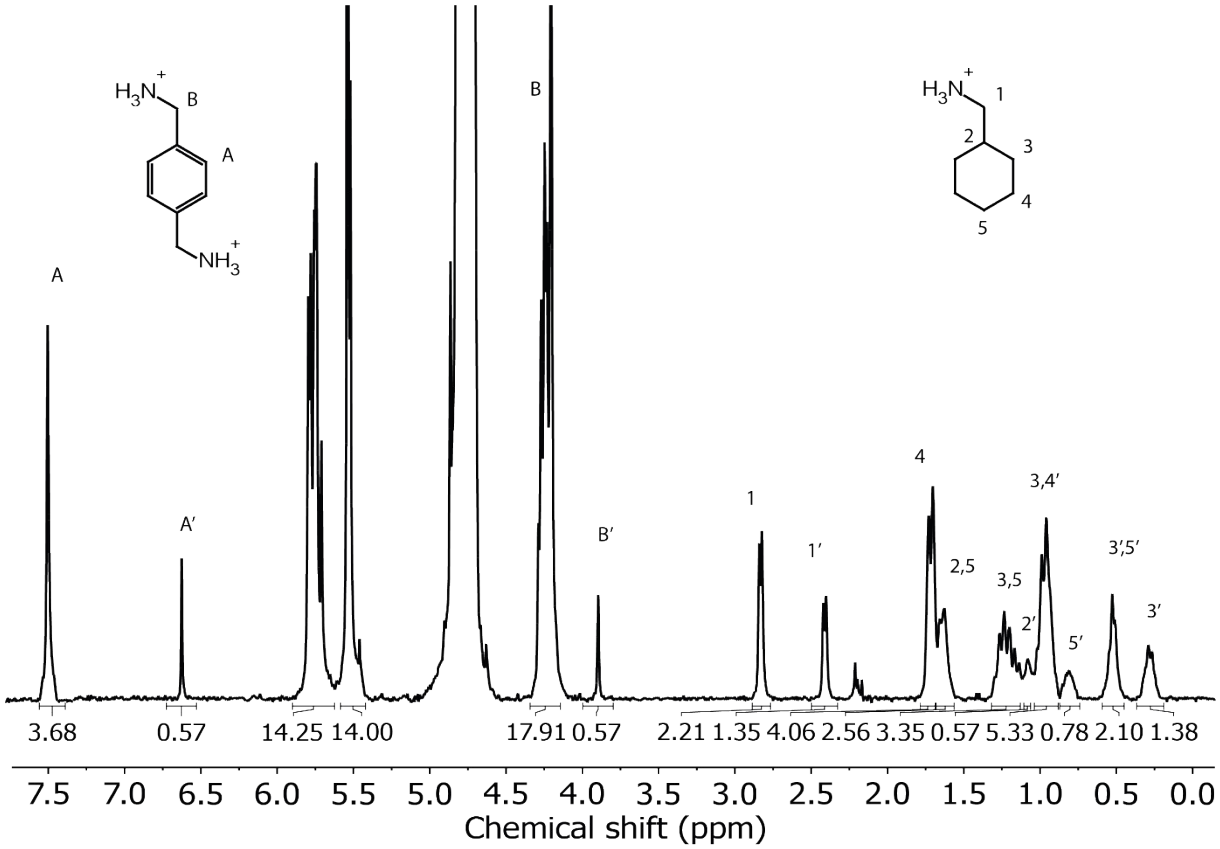

Fig. S21 ^{1}H NMR spectra used to determine the K_{rel} for PXD•CB7 and CHMA•CB7 in D_2O at pD 7.4. Concentrations were 1.10 mM PXD, 1.86 mM CHMA and 1 mM CB7.

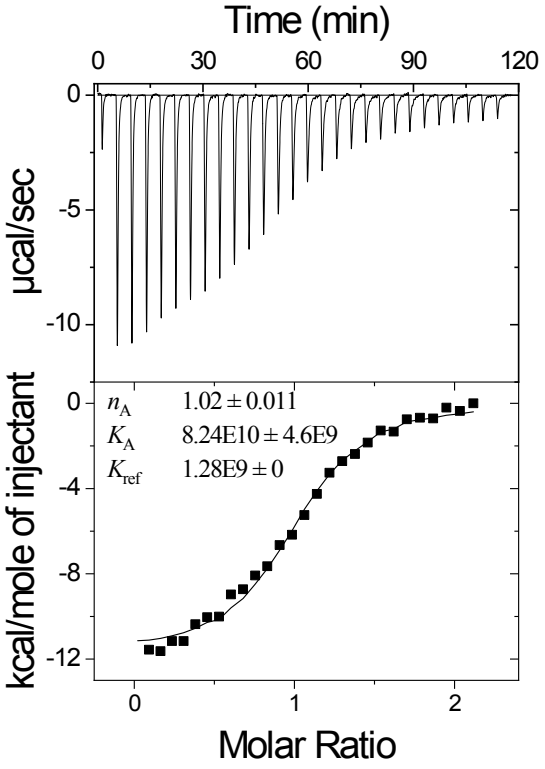

Fig. S22 Competition ITC isotherms on complexation of 250 µM CB7 with CHMA in the prescnce of 1.0 mM HMD in H_2O, pH 7.0, 25 °C.

4.7 *cis*-1,4-Bis(aminomethyl)-cyclohexane (CBAMC)

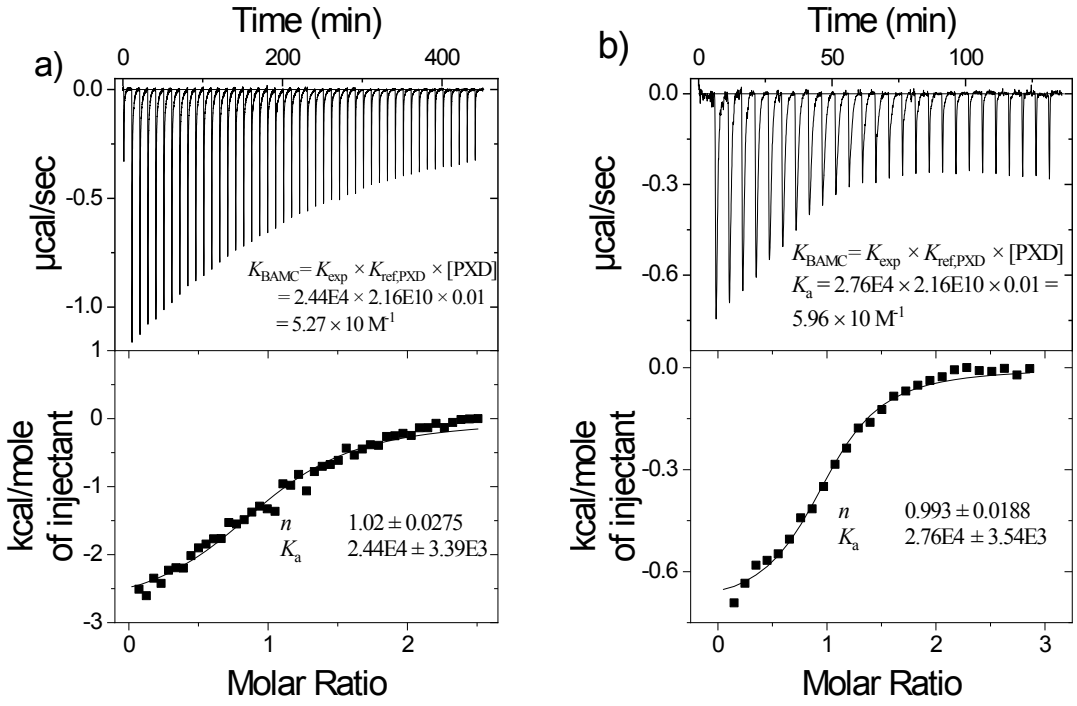

Fig. S23 Competition ITC experiments on complexation of a) 0.25 mM and b) 0.20 mM CB7 with CBAMC with in the presence of 10 mM PXD at pH 7.0, 25 °C.

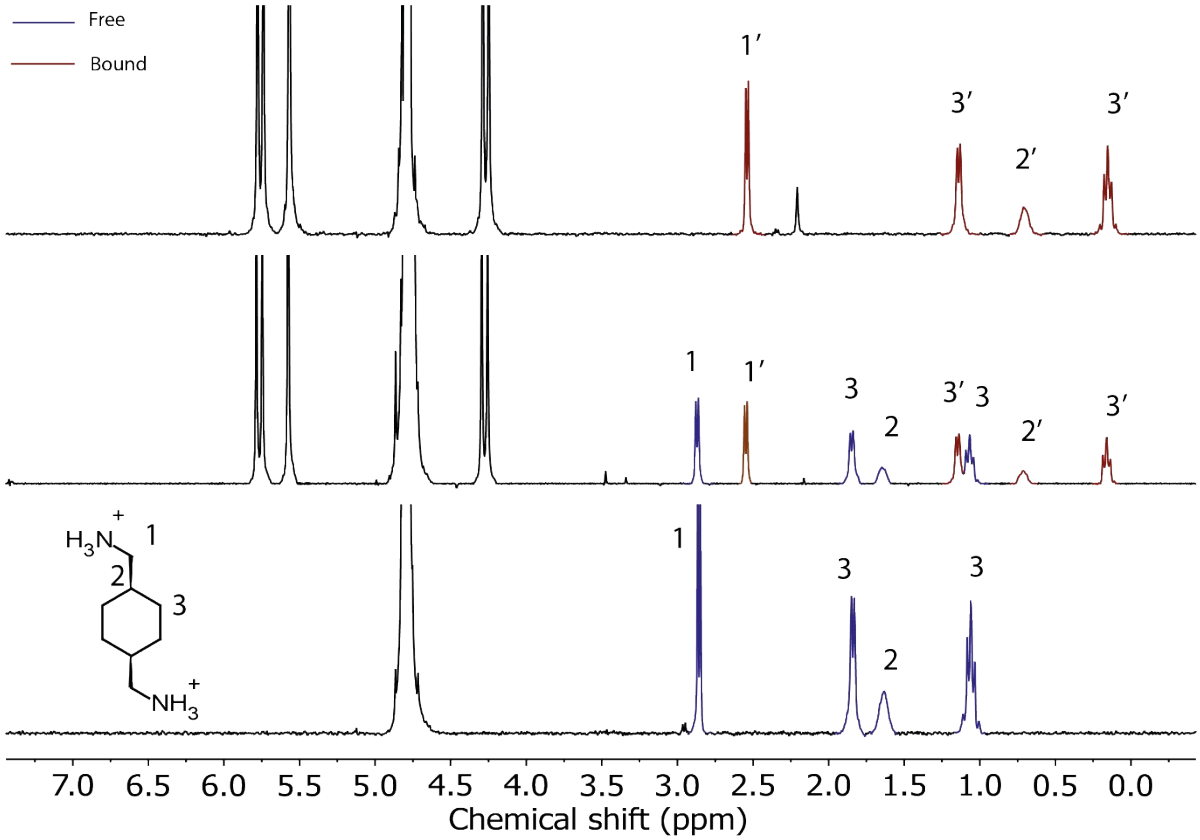

Fig. S24 ^{1}H NMR spectra for 2 mM CBAMC free (bottom), 1 mM CBAMC with 0.5 mM CB7 (middle), and 1 mM CBAMC with 1 mM CB7 (top).

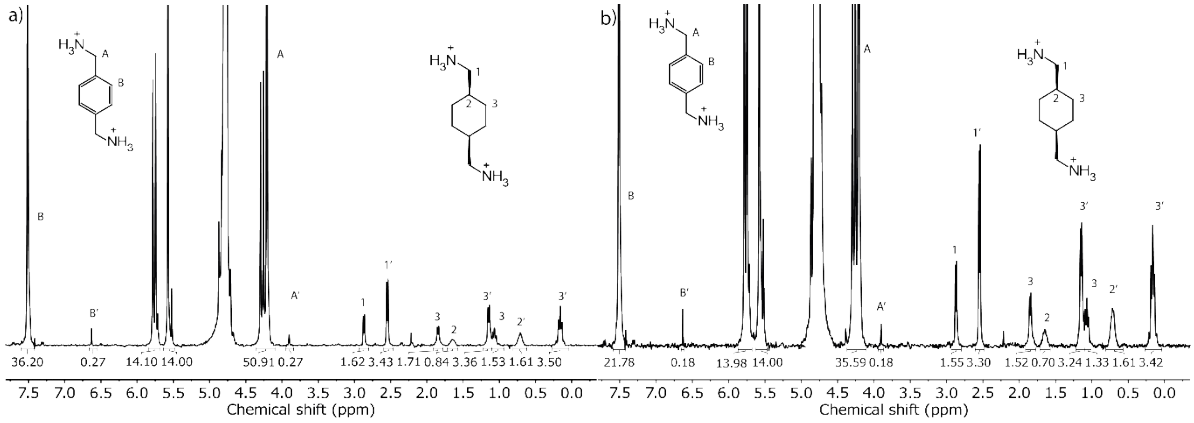

Fig. S25 ^{1}H NMR spectra used to determine the K_{rel} for PXD•CB7 and CBAMC•CB7 in D_2O at pD 7.4. Concentrations were a) 9.2 mM PXD, 1.26 mM CBAMC and 1 mM CB7, b) 5.49 mM PXD, 1.21 mM CBAMC and 1 mM CB7

4.8 (2,3-Diazabicyclo[2.2.2]oct-2-enyl) methylamine (DBO-A)

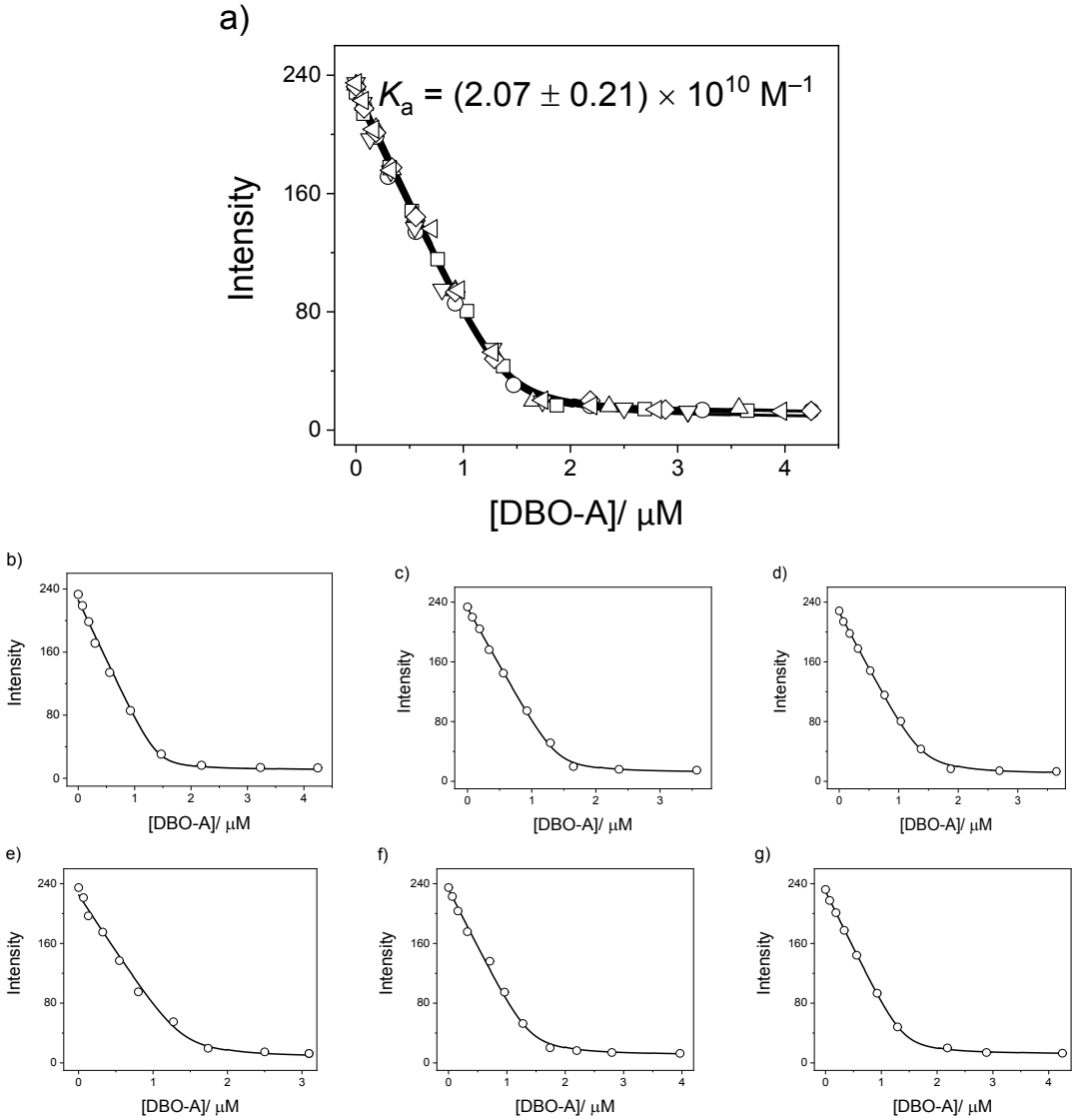

Fig. S26 a) Global fitting of the titration plots shown in Panels b-g. b-g) Titration plots obtained from the fluorescence spectral changes (λ_{ex} = 420 nm, λ_{em} = 490 nm) of 25.0 μM BE and 1.4 μM CB7 upon addition of DBO-A at pH 7.0 in Millipore water in b), c) and d), and in water distilled from $KMnO_4$ in e), f) and g).

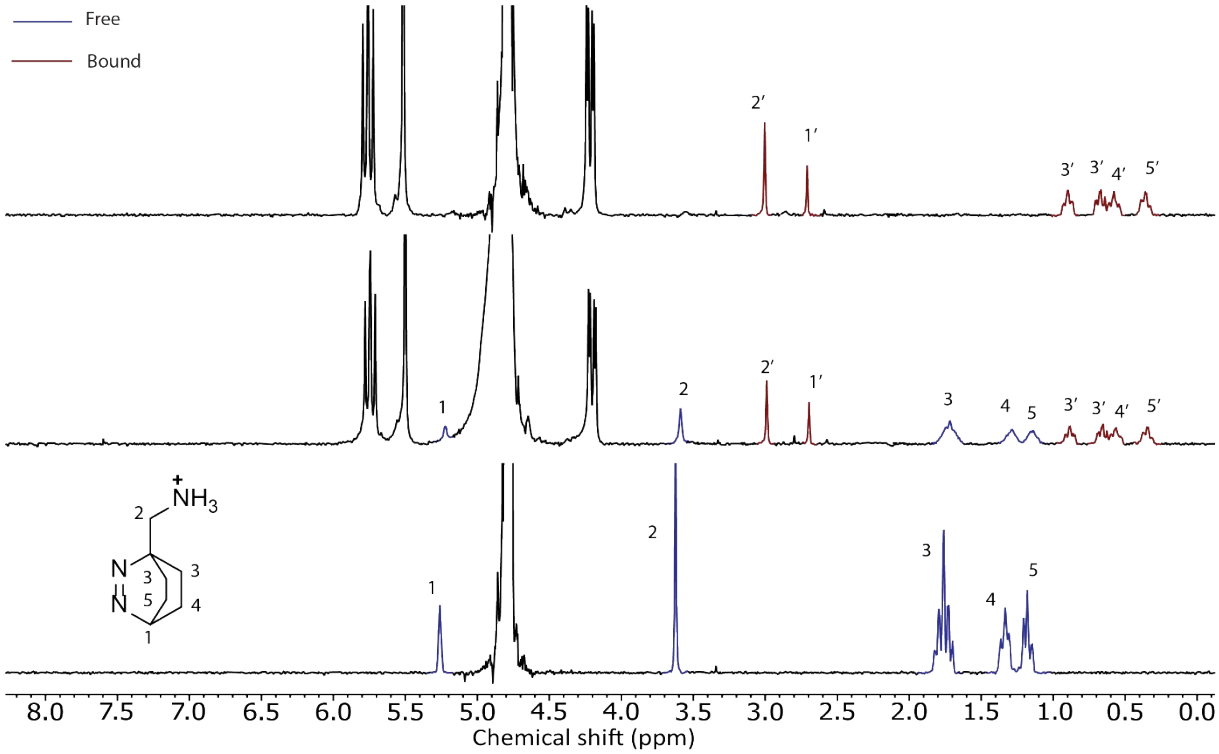

Fig. S27 ^{1}H NMR spectra for 2 mM DBO-A (bottom), 1 mM DBO-A with 0.5 mM CB7 (middle), and 1 mM DBO-A with 1 mM CB7 (top).

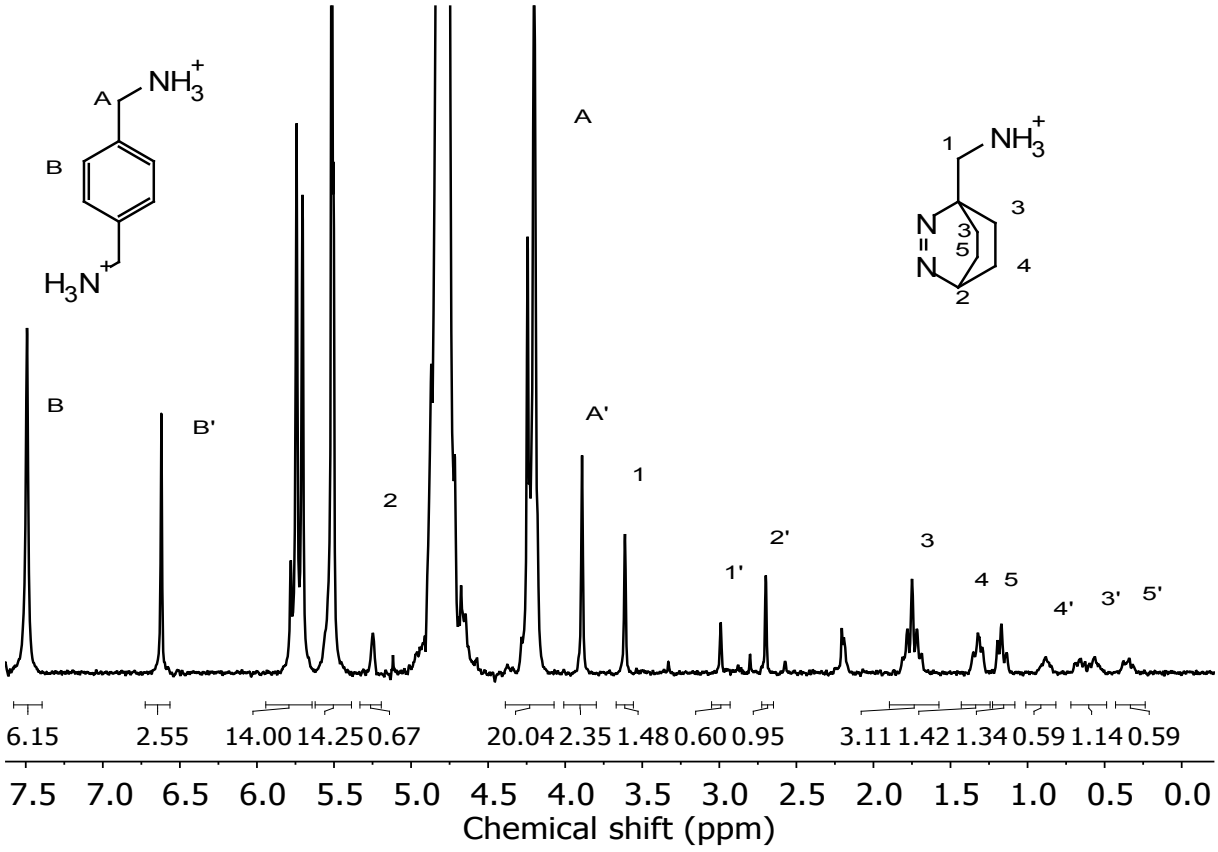

Fig. S28 ^{1}H NMR spectra used to determine the K_{rel} for PXD•CB7 and DBO-A•CB7 in D_2O at pD 7.4. Concentrations were 2.18 mM PXD, 1.15 mM DBO-A and 1 mM CB7.

4.9 Adamantylamine (ADA)

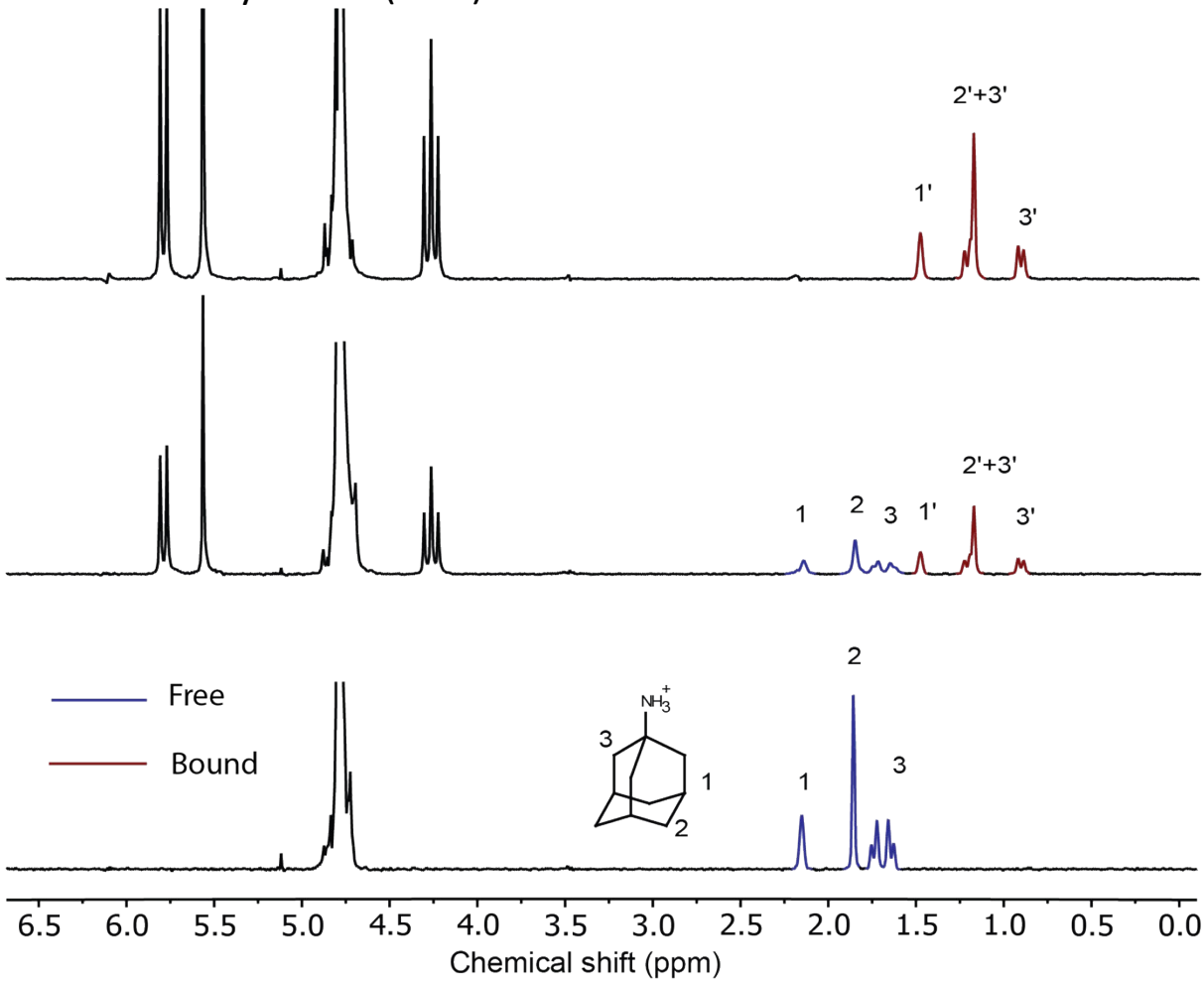

Fig. S29 ^{1}H NMR spectra for 2 mM ADA (bottom), 1 mM ADA with 0.5 mM CB7 (middle), and 1 mM ADA with 1 mM CB7 (top).

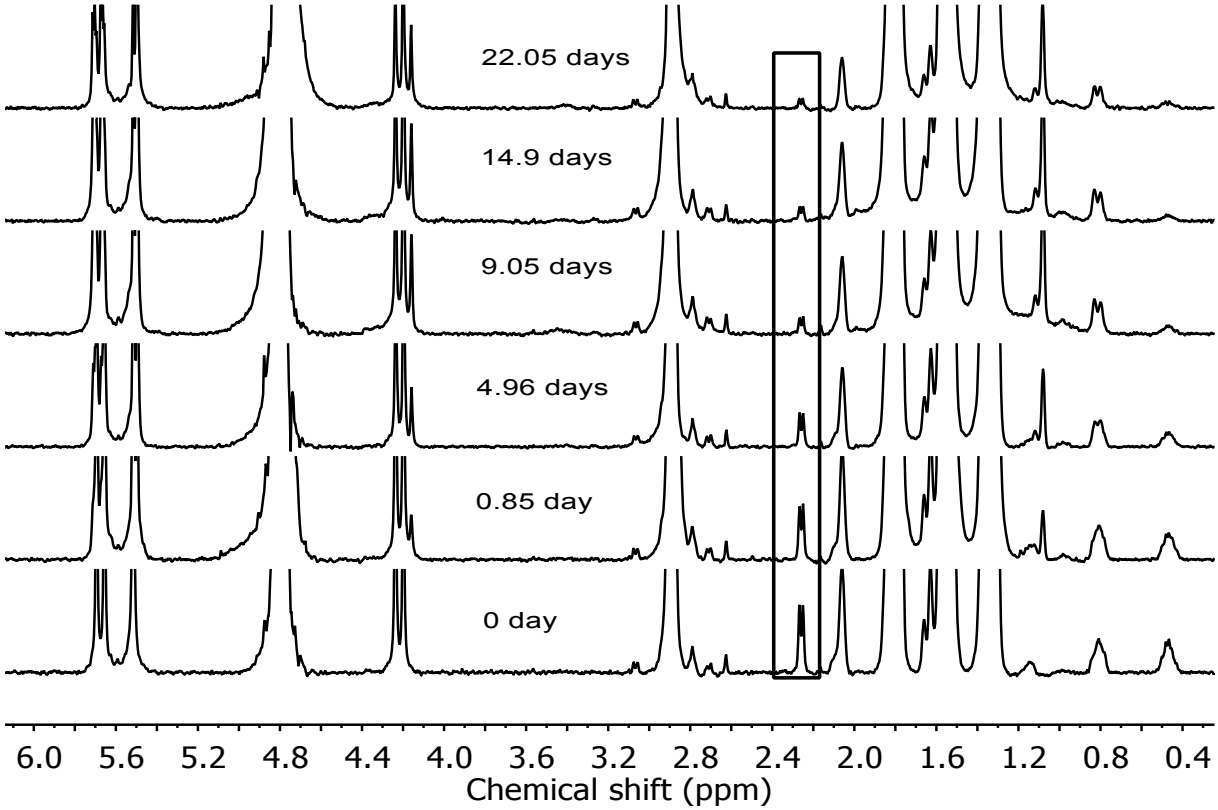

Fig. S30 Time-dependent changes in ^{1}H NMR spectra of 0.74 mM CB7 and 20 mM BAMC after the addition of 0.74 mM ADA at pD 7.4.

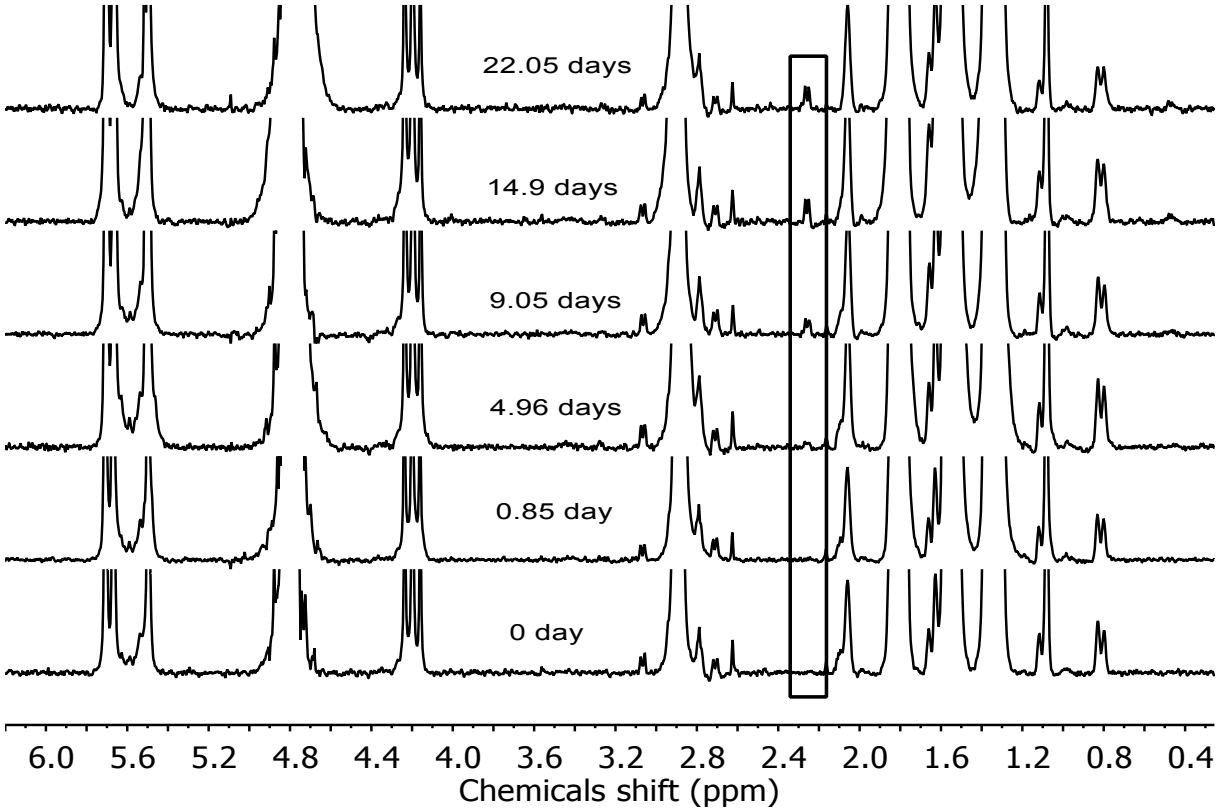

Fig. S31 Time-dependent changes in ^{1}H NMR spectra of 0.74 mM CB7 and 0.74 mM ADA after the addition of 20 mM BAMC at pD 7.4.

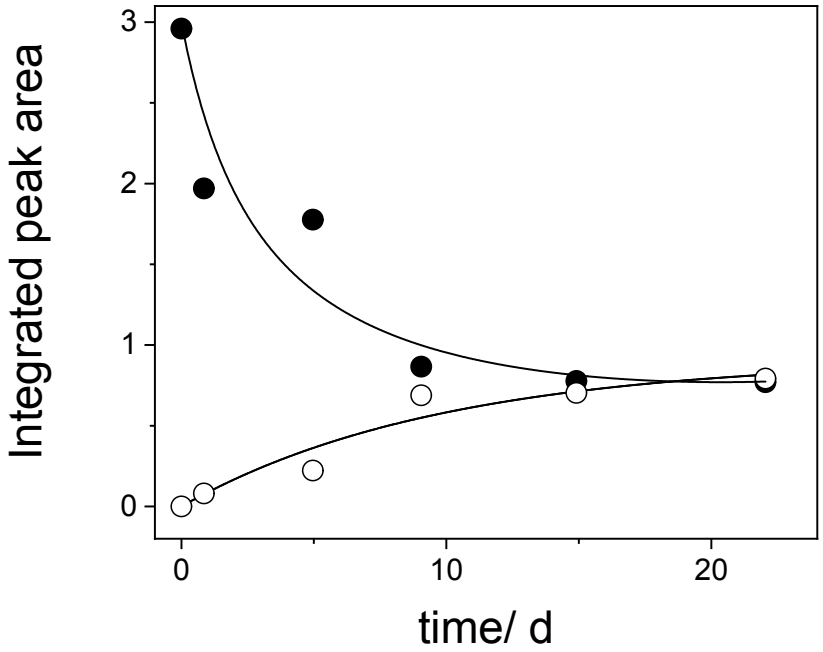

Fig. S32 Time-dependent changes in the integrated peak area of the peak at 2.26 ppm assigned to the BAMC complex. The upper curve (●) was obtained with 0.74 mM CB7 and 20 mM BAMC after the addition of 0.74 mM ADA (Fig. S30) and the lower curve (○) with 0.74 mM CB7 and 0.74 mM ADA after the addition of 20 mM BAMC (Fig. S31). The lines were inserted to guide the eye.

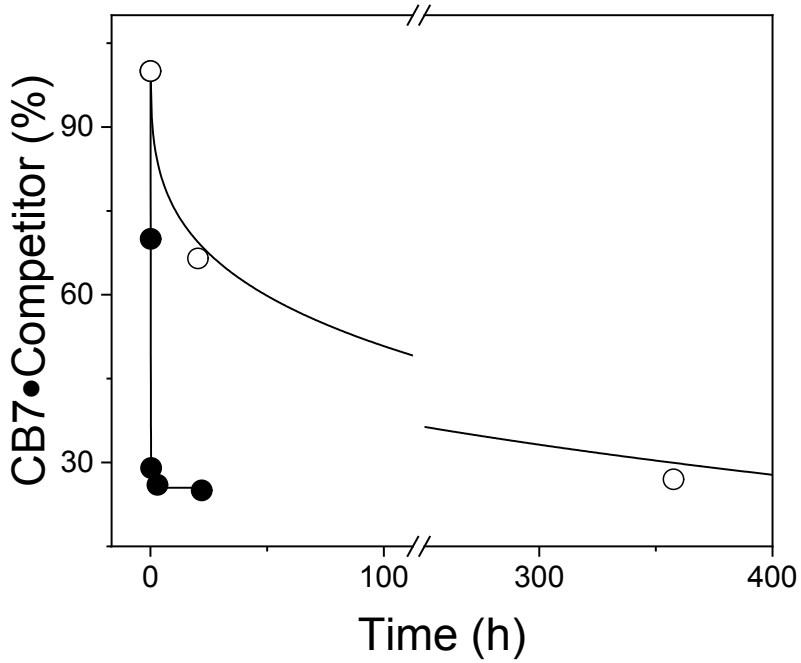

Fig. S33 Dissociation of the pre-formed CBAMC•CB7 (○) and FDMA•CB7 (●) complexes. Therefore, 20 mM CBAMC and 0.74 mM CB7 or 17 mM FDMA and 1 mM CB7 were mixed and 1.25 mM ADA leading to dissociation of the complexes by competitive binding. The lines were inserted to guide the eye.

4.10 Aminomethyladamantane (AMADA)

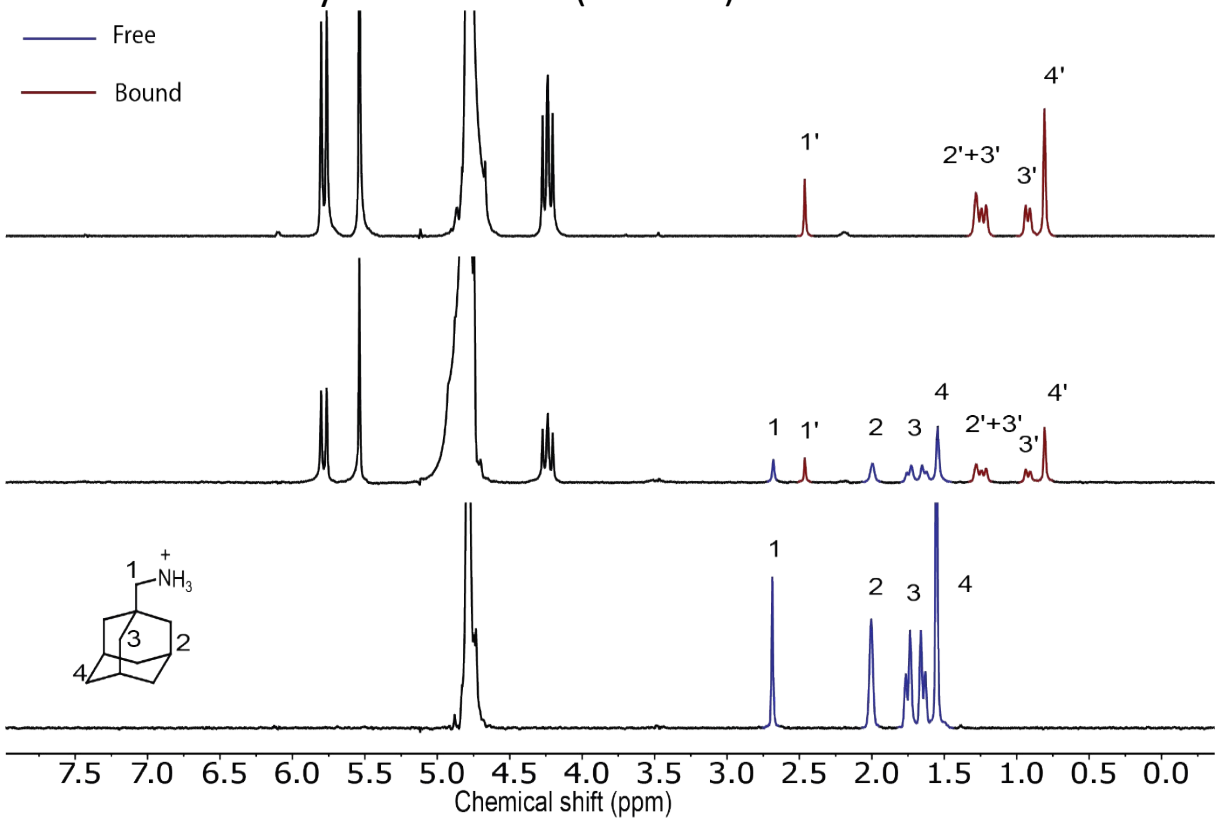

Fig. S34 ^{1}H NMR spectra for 2 mM AMADA (bottom), 1 mM AMADA with 0.5 mM CB7 (middle), and 1 mM AMADA with 1 mM CB7 (top).

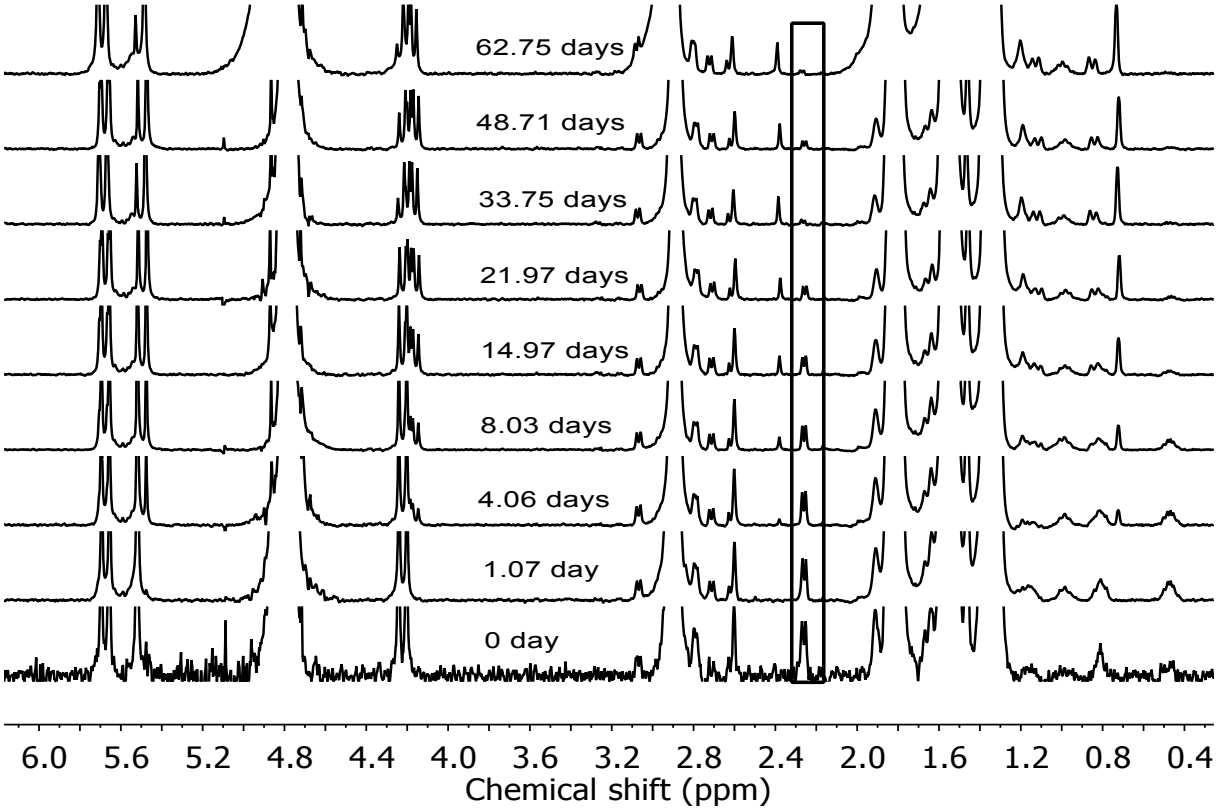

Fig. S35 Time-dependent changes in ^{1}H NMR spectra of 0.56 mM of CB7 and 40 mM BAMC after addition of 0.56 mM AMADA at pD 7.4.

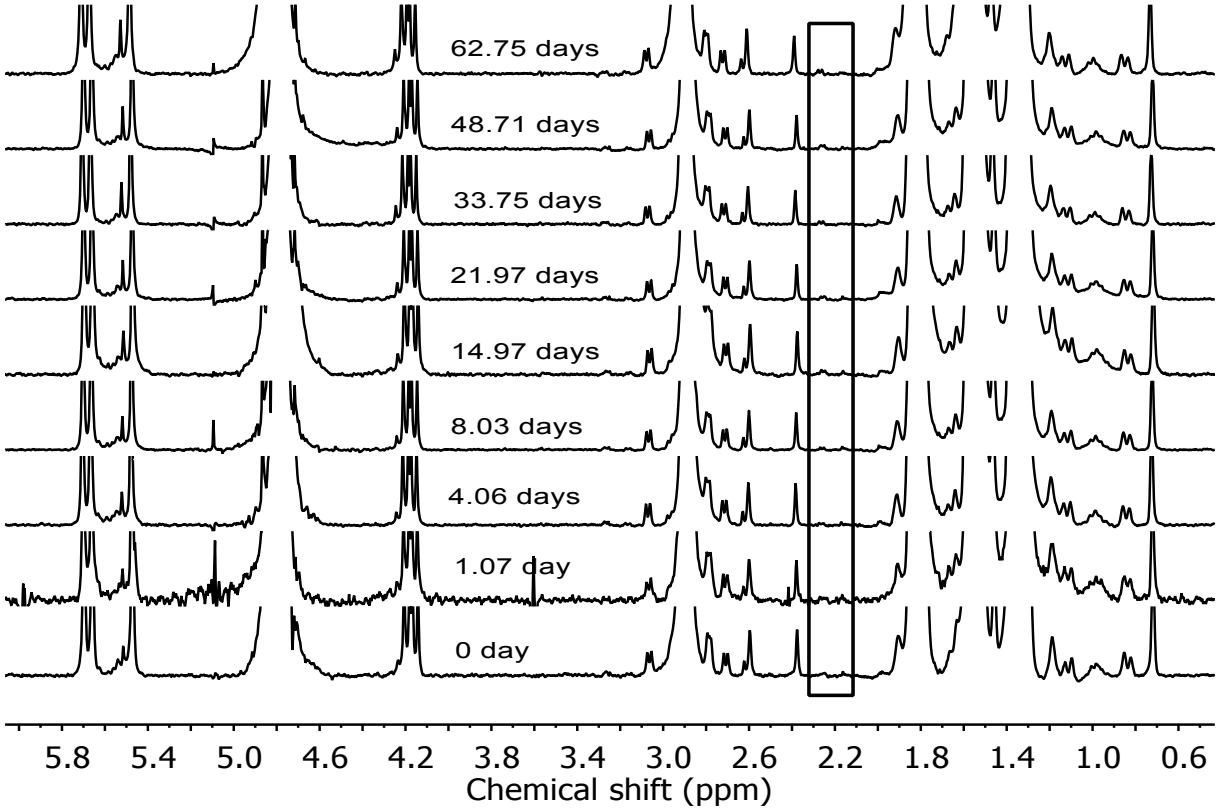

Fig. S36 Time-dependent changes in ^{1}H NMR spectra of 0.56 mM of CB7 and 0.56 mM AMADA after addition of 40 mM BAMC at pD 7.4.

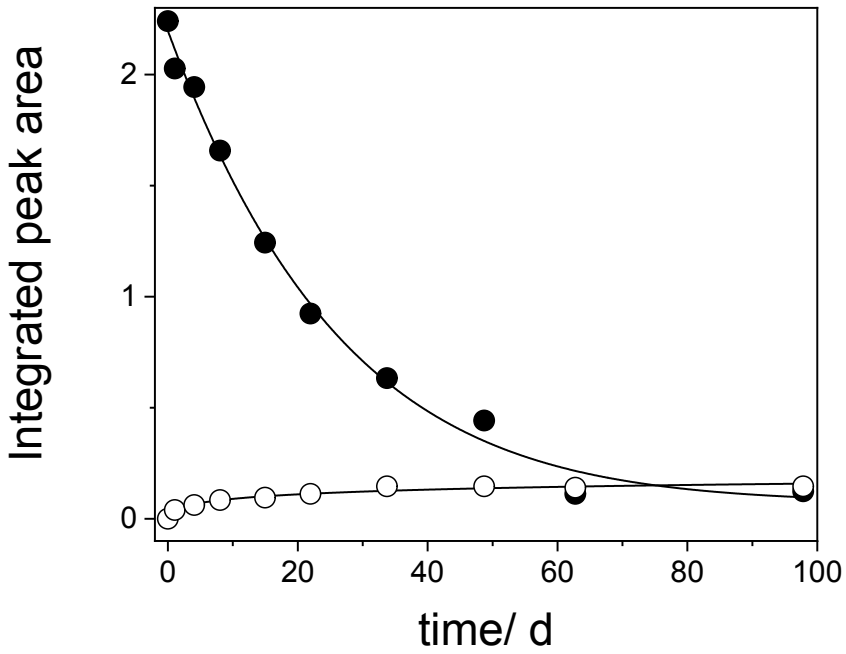

Fig. S37 Time-dependent changes in the integrated peak area of the BAMC•CB7 complex peak at 2.26 ppm. The upper curve (●) was obtained with 0.56 mM CB7 and 40 mM BAMC after the addition of 0.56 mM ADA (Fig. S35) and the lower curve (○) with 0.56 mM CB7 and

0.56 mM ADA after the addition of 40 mM BAMC (Fig. S36). The lines were inserted to guide the eye.

4.11 *N*,*N*-Dimethylaminomethylferrocene (FDMA)

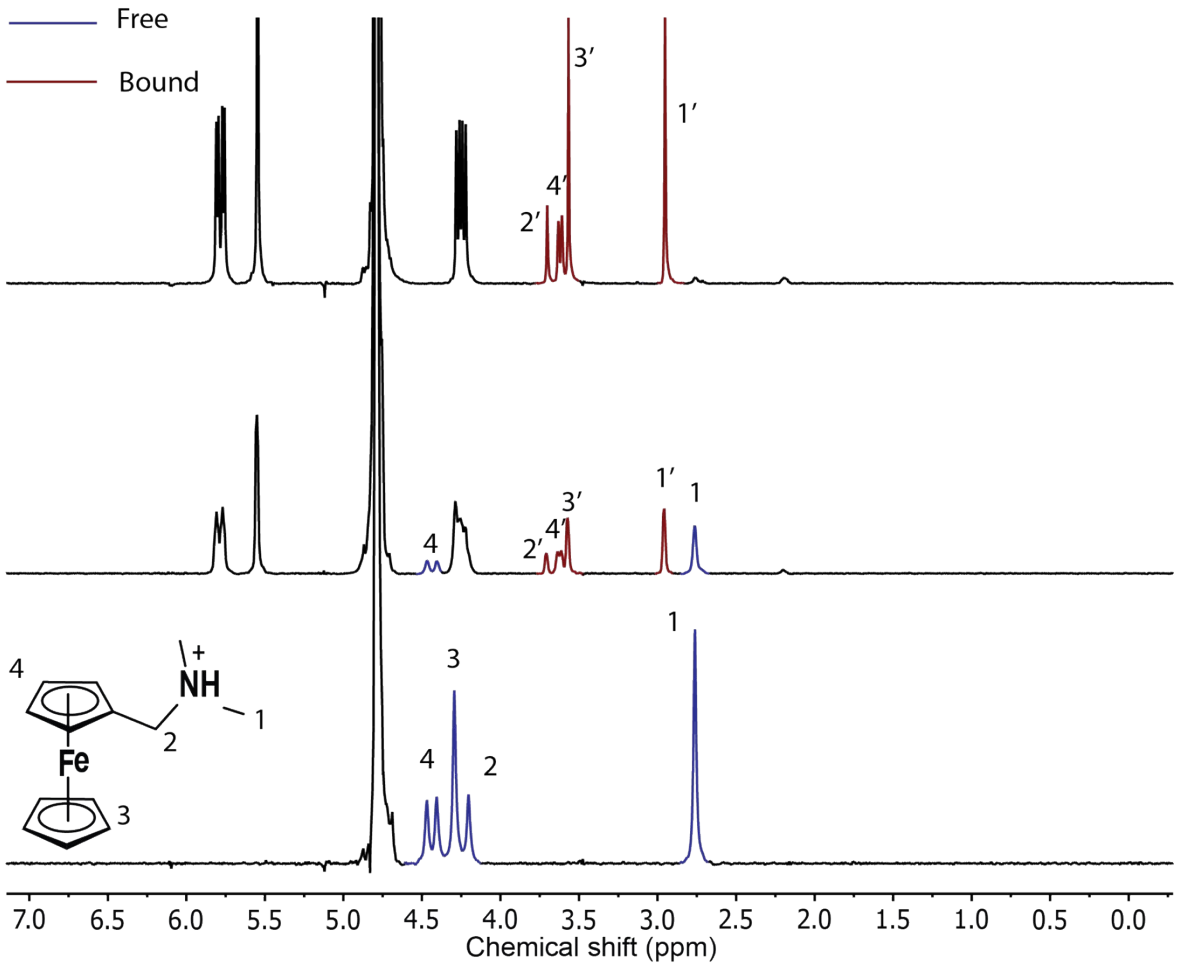

Fig. S38 ^{1}H NMR spectra of 2 mM FDMA (bottom), 1 mM FDMA with 0.5 mM CB7 (middle), and 1 mM FDMA with 1 mM CB7 (top).

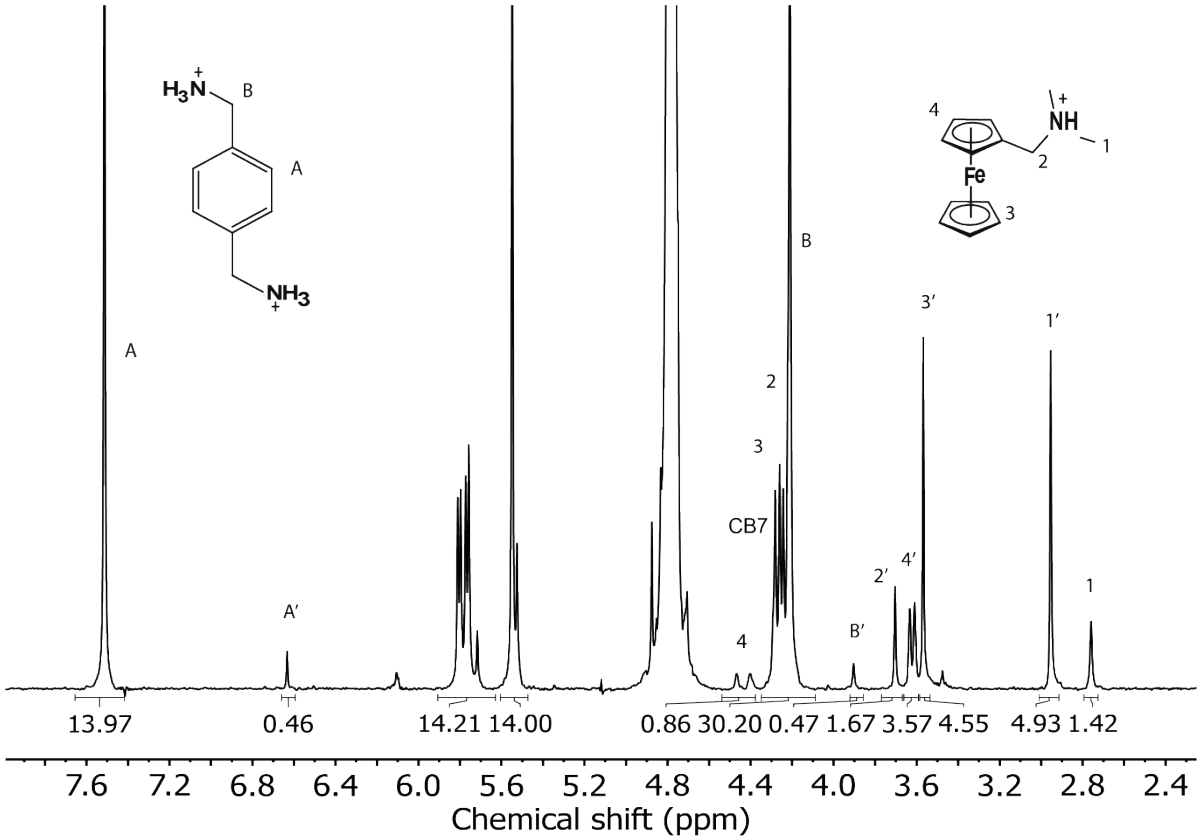

Fig. S39 ^{1}H NMR spectra used to determine the K_{rel} for PXD•CB7 and FDMA•CB7 in D_2O at pD 7.4. Concentrations were 3.5 mM PXD, 1.06 mM FDMA and 1 mM CB7.

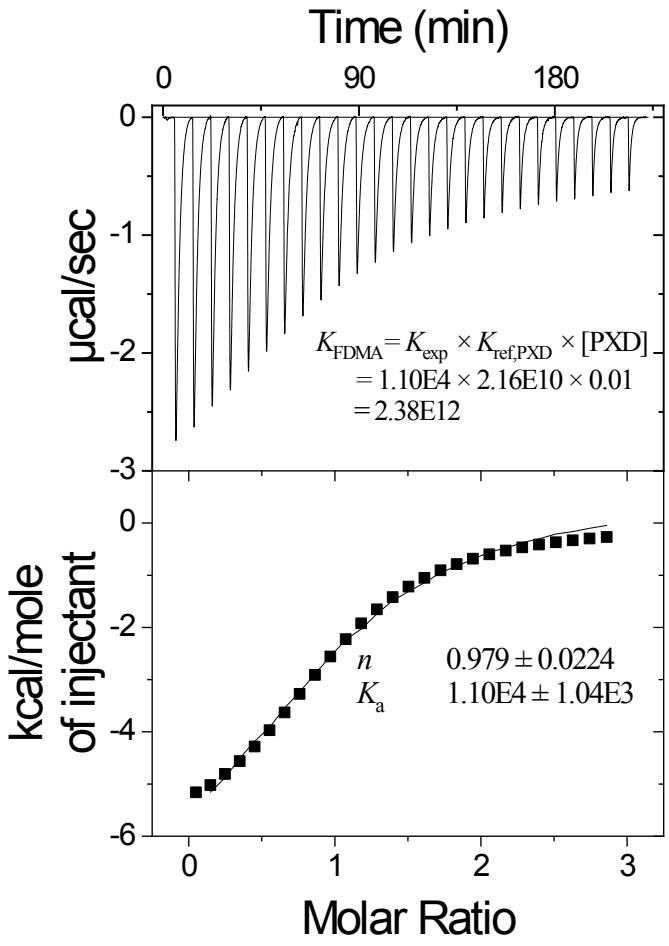

Fig. S40 Competition ITC experiments on complexation of 0.43 mM CB7 and 10 mM PXD with FDMA as competitor at pH 7.0, 25 °C.

4.12 (*S*)-2-(Adamantan-1-yl)-2-aminoacetic acid (AMADA-aa)

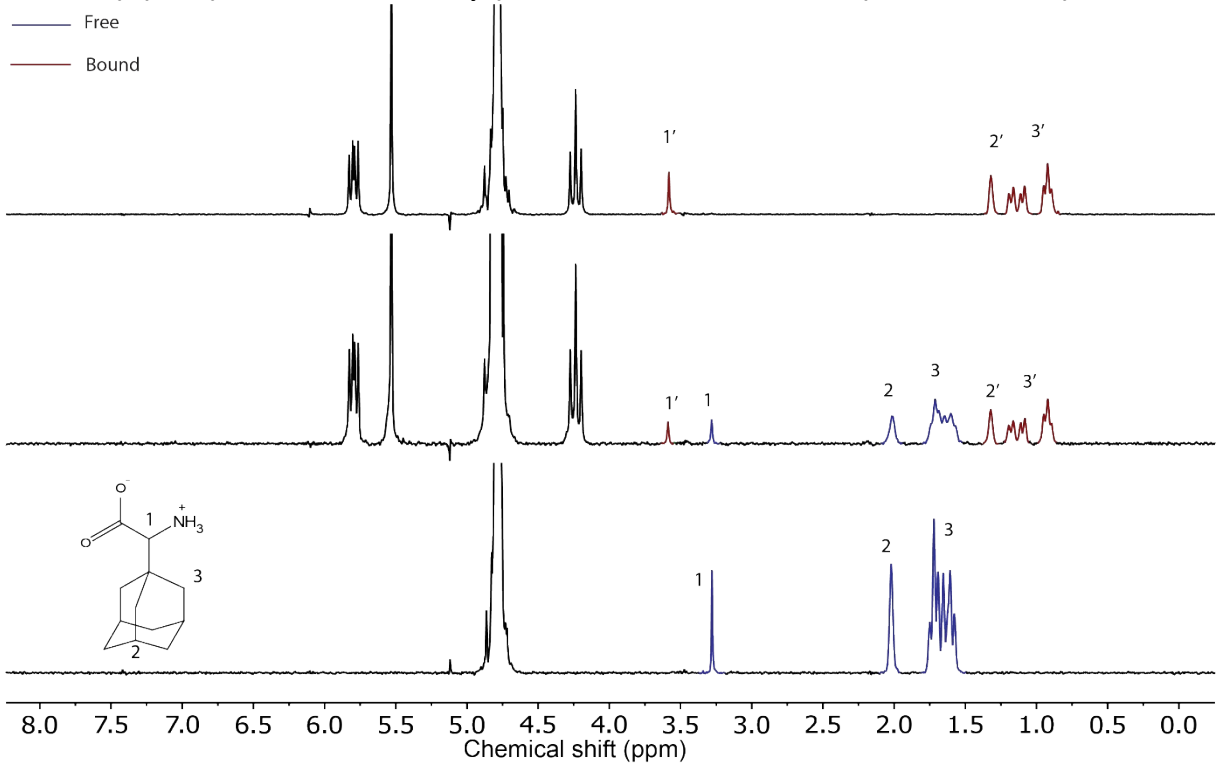

Fig. S41 ^{1}H NMR spectra of 2 mM AMADA-aa (bottom), 1 mM AMADA-aa with 0.5 mM CB7 (middle), and 1 mM AMADA-aa with 1 mM CB7 (top).

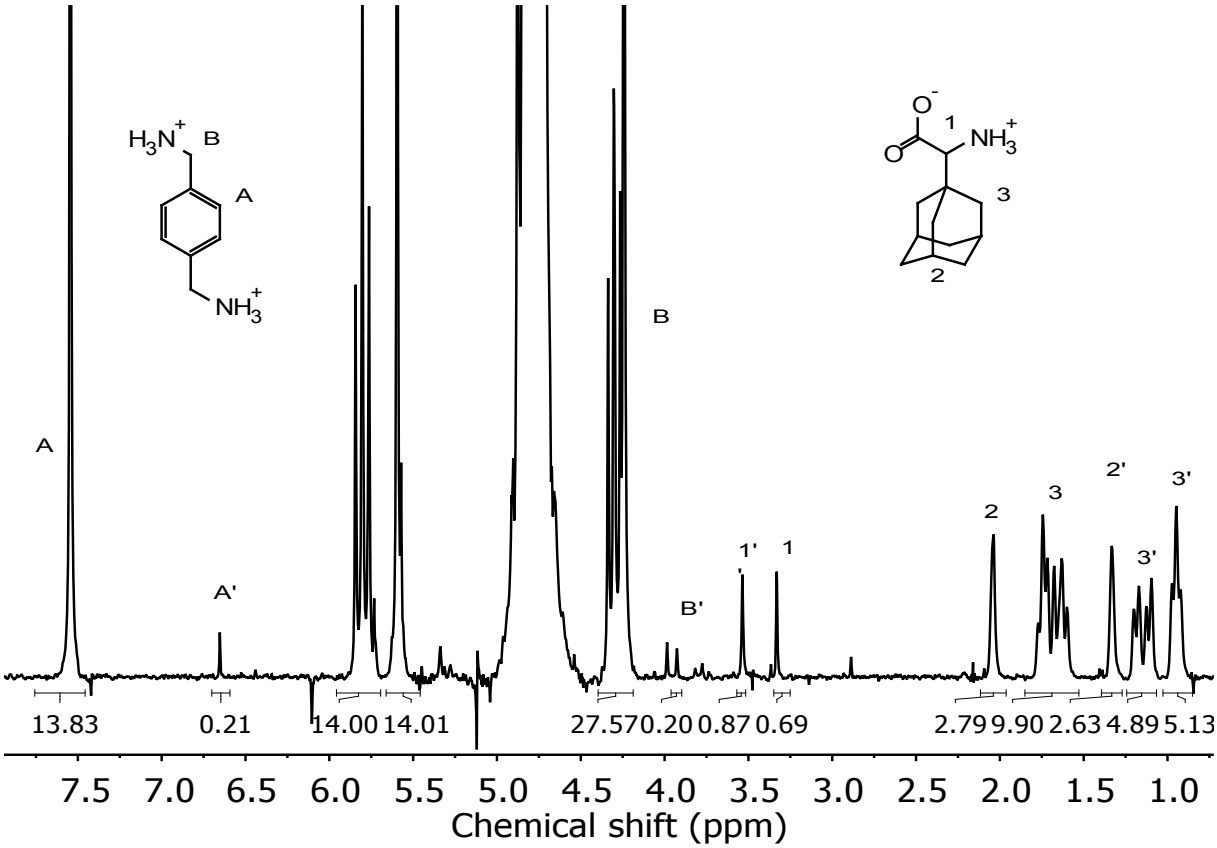

Fig. S42 ^{1}H NMR spectra used to determine the K_{rel} for PXD•CB7 and AMADA-aa•CB7 in D_2O at pD 7.4. Concentrations were 3.5 mM PXD, 1.65 mM FDMA and 1 mM CB7.

4.13 Aminomethyladamantane-putrescine (AMADA-Put)

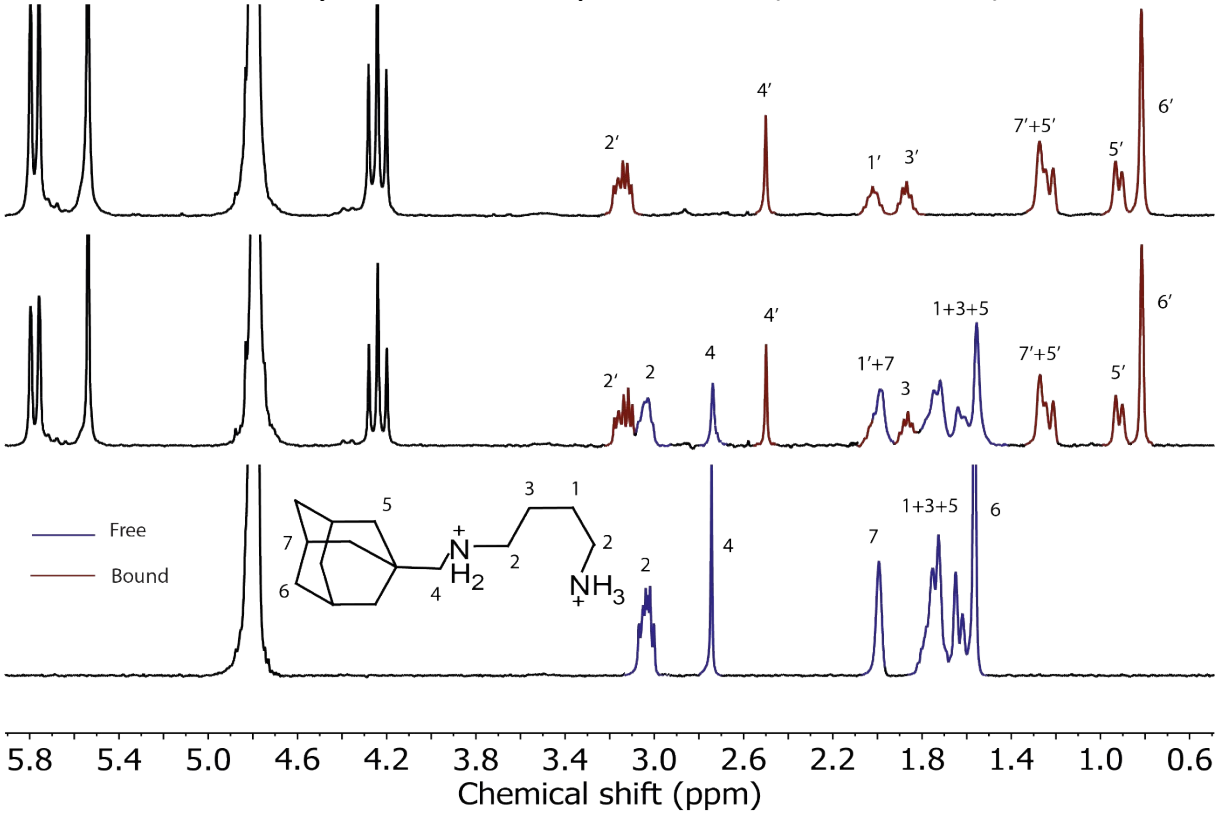

Fig. S43 ^{1}H NMR spectra for 2 mM AMADA-Put (bottom), 1 mM AMADA-Put with 0.5 mM CB7 (middle), and 1 mM AMADA-Put with 1 mM CB7 (top).

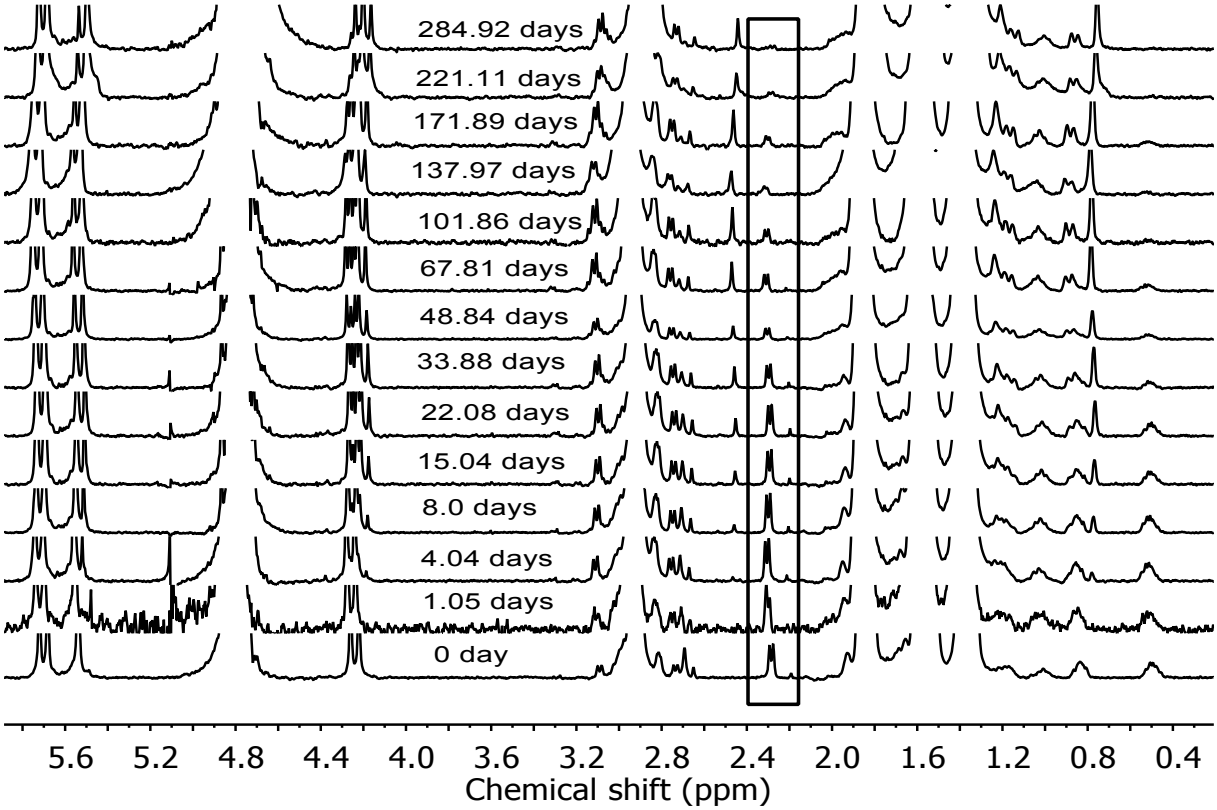

Fig. S44 Time-dependent changes in ^{1}H NMR spectra of 0.56 mM of CB7 and 50 mM BAMC after addition of 0.93 mM AMADA-Put at pD 7.4.

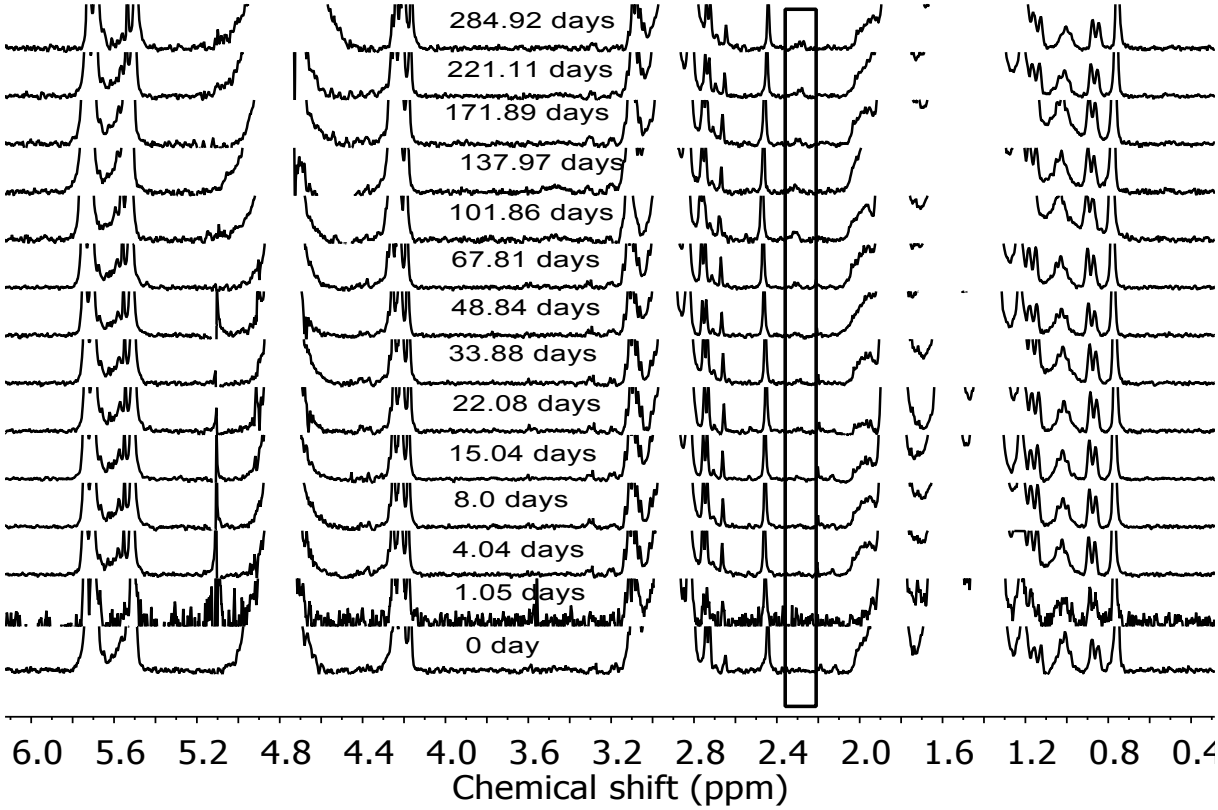

Fig. S45 Time-dependent changes in ^{1}H NMR spectra of 0.56 mM CB7 and 0.93 mM AMADA-Put after addition of 50 mM BAMC at pD 7.4.

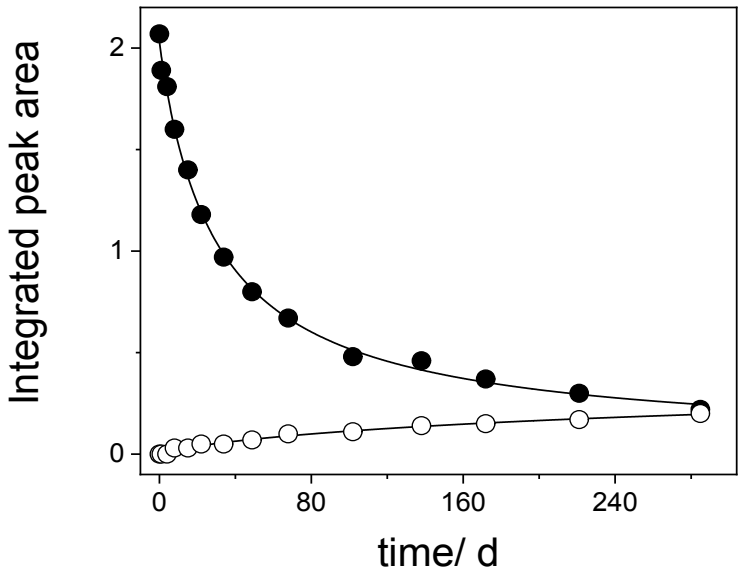

Fig. S46 Time-dependent changes in the integrated peak area of the BAMC•CB7 complex peak at 2.26 ppm. The upper curve (●) was obtained with 0.56 mM CB7 and 50 mM BAMC after the addition of 0.93 mM AMADA-Put (Fig. S44) and the lower curve (○) with 0.56 mM

CB7 and 0.93 mM AMADA-Put after the addition of 50 mM BAMC (Fig. S45). The lines were inserted to guide the eye.

4.14 *trans*-1,4-Bis(aminomethyl)-cyclohexane (TBAMC)

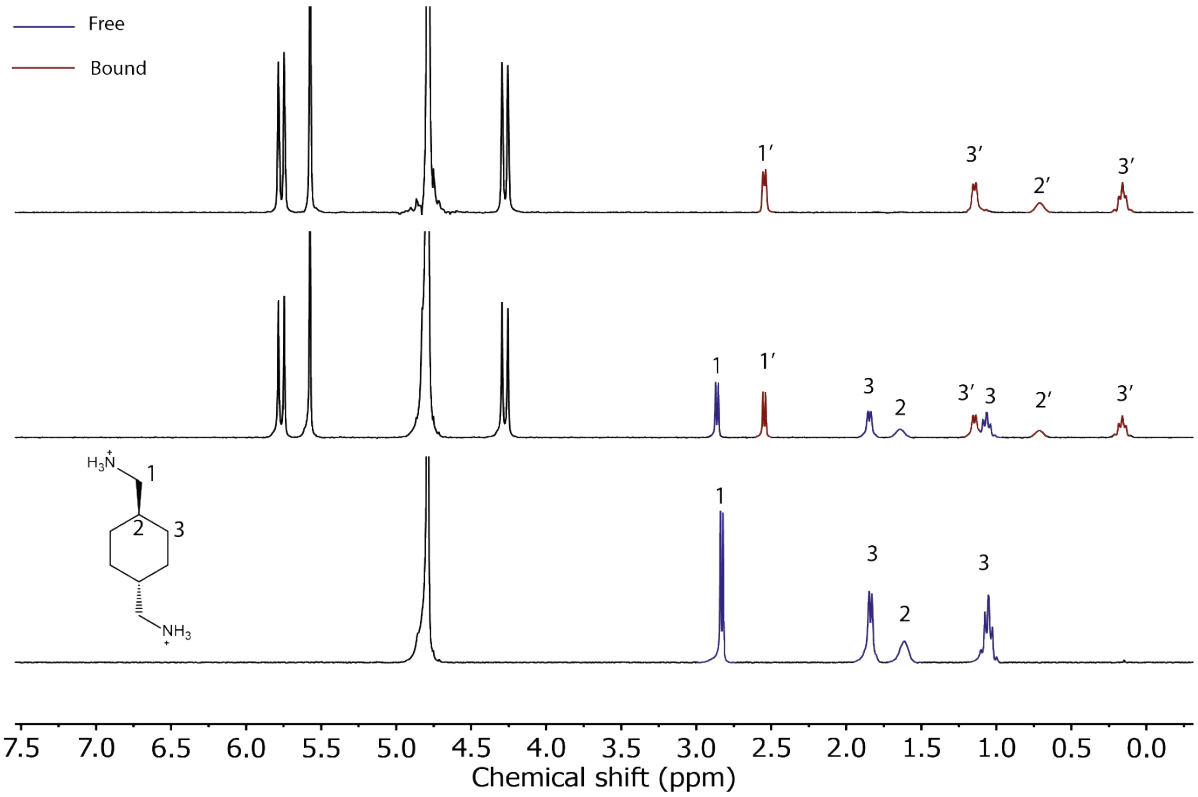

Fig. S47 ^{1}H NMR spectra for 2 mM TBAMC free (bottom), 1 mM TBAMC with 0.5 mM CB7 (middle), and 1 mM TBAMC with 1 mM CB7 (top).

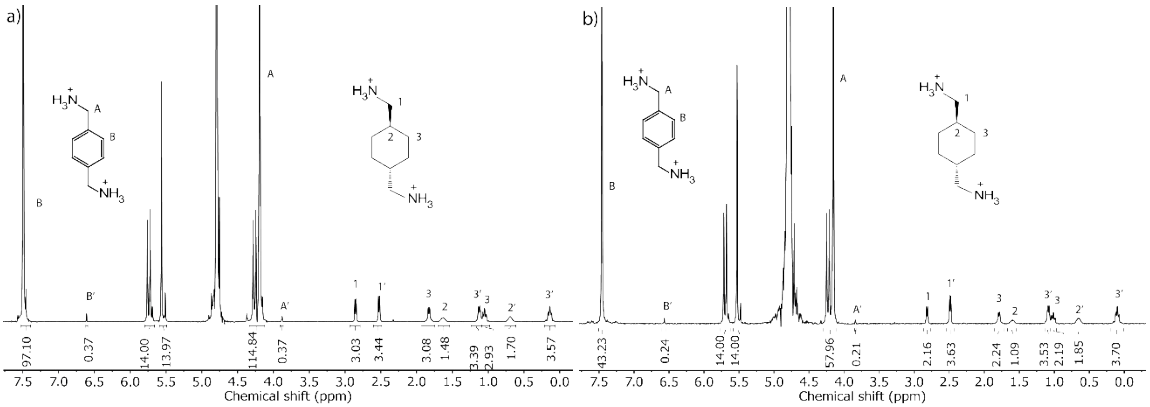

Fig. S48 ^{1}H NMR spectra used to determine the K_{rel} for PXD•CB7 and TBAMC•CB7 in D_2O at pD 7.4. Concentrations were a) 20 mM PXD, 1.6 mM TBAMC, and 1 mM CB7 and b) 10.8 mM PXD, 1.47 mM TBAMC, and 1 mM CB7.

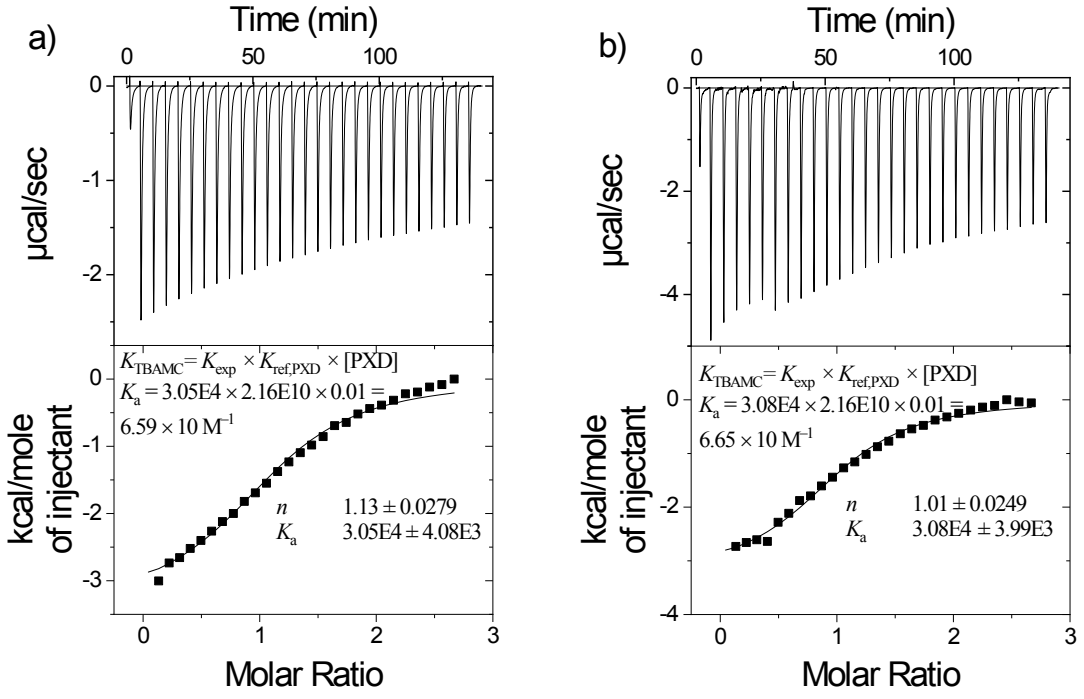

Fig. S49 Competition ITC experiments on complexation of TBAMC with a) 0.25 mM CB7 or b) 0.20 mM CB7 in the presence of 10 mM PXD at pH 7.0, 25 °C.

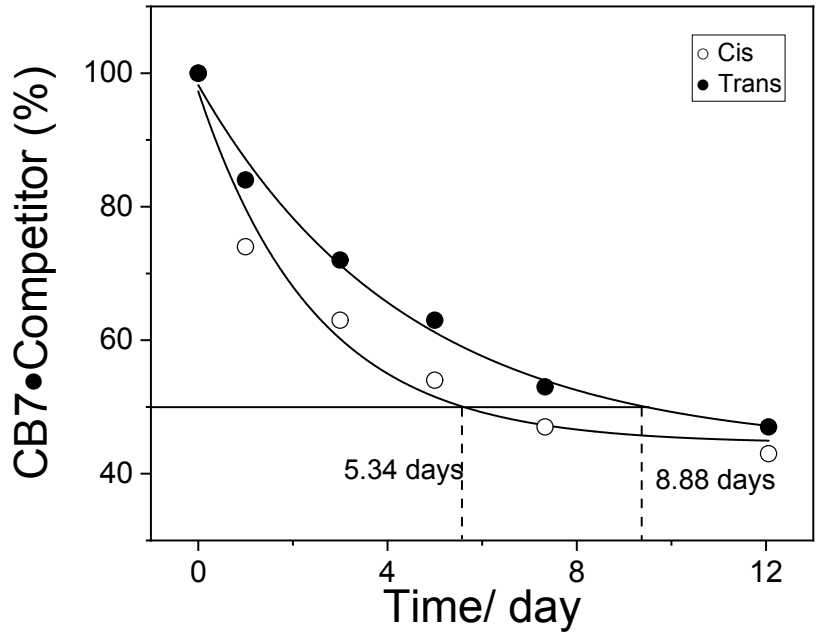

Fig. S50 Approximation of the half-life times of the CB7 complexes of CBAMC (○), and TBAMC (●). The fraction of initial CB7 complex was monitored as a function of time with 1 mM CB7 with 33 mM CBAMC (○) and 1 mM CB7 33 mM TBAMC (●) followed by addition of 1.25 mM ADA. The lines were inserted to guide the eye.

5. References

1 C. Marquez, F. Huang and W. M. Nau, *IEEE Trans. Nanobiosci*, 2004, **3**, 39-45.

2 R. R. Hudgins, F. Huang, G. Gramlich and W. M. Nau, *J. Am. Chem. Soc.*, 2002, **124**, 556-564.

3 A. Hennig, A. Hoffmann, H. Borcherding, T. Thiele, U. Schedler and U. Resch-Genger, *Chem. Commun.*, 2011, **47**, 7842-7844.

4 P. K. Glasoe and F. A. Long, *J. Phys. Chem.*, 1960, **64**, 188-190.

5 A. Hennig and W. M. Nau, *Front. Chem.*, 2020, **8**.

6 P. Thordarson, *Chem. Soc. Rev.*, 2011, **40**, 1305-1323.

7 P. R. Bevington, & Robinson, D. K., *Data reduction and error analysis for the physical sciences*, New York: McGraw-Hill., 2003.